Received: 14 April 2022 | Accepted: 27 September 2022

DOI: 10.1002/ajb2.16084

RESEARCH ARTICLE

Botany

Phylogenomics and plastome evolution of a Brazilian mycoheterotrophic orchid, *Pogoniopsis schenckii*

Nathaniel J. Klimpert[1] | **Juliana Lischka Sampaio Mayer**[2] | **Deise Schroder Sarzi**[3] | **Francisco Prosdocimi**[3] | **Fábio Pinheiro**[2] | **Sean W. Graham**[1]

[1]Department of Botany, University of British Columbia, 6270 University Boulevard, Vancouver, British Columbia V6T 1Z4, Canada

[2]Departamento de Biologia Vegetal, Universidade Estadual de Campinas, 255 Rua Monteiro Lobato, Campinas, São Paulo, 13.083-862, Brazil

[3]Laboratório de Genômica e Biodiversidade, Instituto de Bioquímica Médica Leopoldo de Meis, Universidade Federal Do Rio de Janeiro, UFRJ/CCS/Bloco B33, Rio de Janeiro, RJ, 21.941-902, Brazil

Correspondence

Sean W. Graham, Department of Botany, University of British Columbia, 6270 University Boulevard, Vancouver, British Columbia, V6T 1Z4, Canada.
Email: swgraham@interchange.ubc.ca

Abstract

Premise: *Pogoniopsis* likely represents an independent photosynthesis loss in orchids. We use phylogenomic data to better identify the phylogenetic placement of this fully mycoheterotrophic taxon, and investigate its molecular evolution.

Methods: We performed likelihood analysis of plastid and mitochondrial phylogenomic data to localize the position of *Pogoniopsis schenckii* in orchid phylogeny, and investigated the evolution of its plastid genome.

Results: All analyses place *Pogoniopsis* in subfamily Epidendroideae, with strongest support from mitochondrial data, which also place it near tribe Sobralieae with moderately strong support. Extreme rate elevation in *Pogoniopsis* plastid genes broadly depresses branch support; in contrast, mitochondrial genes are only mildly rate elevated and display very modest and localized reductions in bootstrap support. Despite considerable genome reduction, including loss of photosynthesis genes and multiple translation apparatus genes, gene order in *Pogoniopsis* plastomes is identical to related autotrophs, apart from moderately shifted inverted repeat (IR) boundaries. All *cis*-spliced introns have been lost in retained genes. Two plastid genes (*acc*D, *rpl*2) show significant strengthening of purifying selection. A retained plastid tRNA gene (*trn*E-UUC) of *Pogoniopsis* lacks an anticodon; we predict that it no longer functions in translation but retains a secondary role in heme biosynthesis.

Conclusions: Slowly evolving mitochondrial genes clarify the placement of *Pogoniopsis* in orchid phylogeny, a strong contrast with analysis of rate-elevated plastome data. We documented the effects of the novel loss of photosynthesis: for example, despite massive gene loss, its plastome is fully colinear with other orchids, and it displays only moderate shifts in selective pressure in retained genes.

KEYWORDS

bifunctional gene evolution, comparative genomics, *d*N/*d*S analysis, genome reduction, genome structural changes, intron loss, mitogenome, Orchidaceae tree of life, plastid translation apparatus, plastome

Mycoheterotrophic plants derive some or all of their carbon and other nutrients from soil fungal associates (Merckx et al., 2013). Full mycoheterotrophy has evolved repeatedly across land plants with associated losses of photosynthesis. Over half of the origins are thought to have occurred in Orchidaceae (Merckx and Freudenstein, 2010; Merckx et al., 2013), but to date only a subset of the independent transitions to heterotrophy in this family have been characterized with fully sequenced plastid genomes (Delannoy et al., 2011; Logacheva et al., 2011; Barrett and Davis, 2012; Schelkunov et al., 2015; Feng et al., 2016; Huo et al., 2018; Barrett et al., 2019; Kim et al., 2019; Kim et al., 2020; Lee et al., 2020; Z.-H. Li et al., 2020). Sequenced plastid genomes of mycoheterotrophic plants can provide useful phylogenetic information and insights into patterns of genome evolution and changes in selection with the loss of photosynthesis (e.g., Barrett and Davis, 2012; Barrett et al., 2014; Wicke et al., 2016; Graham et al., 2017). Each mycoheterotrophic lineage represents an independent evolutionary experiment in how to survive without sunlight; studying them allows us to infer general vs. lineage-specific correlates of this major evolutionary transition. For example, fully mycoheterotrophic plants are completely reliant on fungi for their carbon, resulting in release of

selective pressure on genes involved in photosynthesis, which are thought to be rapidly pseudogenized or lost in fully mycoheterotrophic taxa (e.g., Barrett and Davis, 2012; Barrett et al., 2014; Graham et al., 2017).

Gene loss and rate elevation in retained genes can pose challenges for devising classification schemes based on molecular phylogenetic data (e.g., Nickrent et al., 2004; Merckx et al., 2009; Lam et al., 2018), which until recently have largely relied on a few photosynthetic plastid genes (*rbc*L and *atp*B) and nuclear 18S rDNA (e.g., APG, 2003, 2009, 2016). Plastid genomes have nonetheless been useful for inferring the local placement of mycoheterotrophic plants in plant phylogeny (e.g., Lam et al., 2018), including multiple orchid lineages (Barrett and Davis, 2012; Givnish et al., 2015; Schelkunov et al., 2015; Lallemand et al., 2019; Li et al., 2019; Kim et al., 2020; Pérez-Escobar et al., 2021; Serna-Sánchez et al., 2021). While the increased adoption of whole-plastome data has improved our understanding of the phylogenetic position of these mycoheterotrophic orchid lineages, several orchid genera with highly rate-elevated plastid genomes—including *Epipogium* (Schelkunov et al., 2015; Lam et al., 2018; Li et al., 2019) and *Rhizanthella* (Delannoy et al., 2011; Lam et al., 2018)—continue to be difficult to place using plastid data alone. The extreme rate elevation in these heterotrophic plants likely reflects an overall higher rate of mutation (e.g., Bromham et al., 2013) and increased tolerance for deleterious mutations (Wicke and Naumann, 2018). Mitochondrial genes usually evolve substantially more slowly than plastid genes in general (e.g., Petersen et al., 2019; Zervas et al., 2019; Lin et al., 2022), and also tend to display lower variation in rate elevation (Wolfe et al., 1987; Drouin et al., 2008). Both features should make them less susceptible to long-branch artifacts (e.g., Felsenstein, 1978; Hendy and Penny, 1989; Kuhner and Felsenstein, 1994; Gaut and Lewis, 1995; Lin et al., 2022). Although mitochondrial phylogenomic data sets have been used relatively rarely in plant phylogenetic studies, they show promise when used either individually or in tandem with plastid data sets for difficult-to-place taxa (e.g., Li et al., 2019; Soto Gomez et al., 2020; Lin et al., 2022).

Observations of repeated gene loss in severely reduced plastid genomes have also contributed to a more complete understanding of the functions of retained genes (e.g., Barbrook et al., 2006; Graham et al., 2017; Su et al., 2019). Fully sequenced genomes also allow us to document changes in purifying selection acting on individual genes (e.g., Logacheva et al., 2011; Lam et al., 2015; Bell et al., 2020; Yudina et al., 2021) and shifts in substitution rate (e.g., Schelkunov et al., 2015; Feng et al., 2016). They also allow us to expand our understanding of the types of genome structural change that are possible (e.g., Lam et al., 2015; Joyce et al., 2018; Yudina et al., 2021). Although plastid genomes are thought to include both circular and linear-branched forms (Bendich, 2004; Oldenburg and Bendich, 2004), they are usually presented in a circular form. The arrangement of genes in green-plant plastid genomes is otherwise generally highly conserved (e.g., Palmer, 1991; Raubeson and Jansen, 2005; Wicke et al., 2011) and typically comprises a quadripartite structure, with two distinct single-copy regions separated by two inverted-repeat (IR) regions (e.g., Palmer and Delwiche, 1998). In contrast, the plastid genomes of heterotrophic plants commonly display substantial structural changes, including large-scale gene pseudogenization/loss events (e.g., Lam et al., 2015; Petersen et al., 2018; Yuan et al., 2018; Barrett et al., 2019; Jost et al., 2020) with consequential genome reduction (e.g., Logacheva et al., 2014; Schelkunov et al., 2015; Naumann et al., 2016). Plastomes of heterotrophic plants are also generally more prone to changes in gene order/direction due to inversions (e.g., Logacheva et al., 2014; Barrett and Kennedy, 2018). Convergent losses of IR regions and reduction of single-copy regions have also occurred (e.g., Schelkunov et al., 2015; Joyce et al., 2018), as have occasional IR expansions (e.g., Schelkunov et al., 2015; Joyce et al., 2018; Z. Li et al., 2020). However, the mitochondrial genomes of heterotrophic plants are less well studied. While several are known to have experienced limited rate elevation in heterotrophic plants (e.g., Bromham et al., 2013; Petersen et al., 2015; Lin et al., 2022), there appears to be little change in most heterotrophic mitogenomes in terms of overall gene content (e.g., Lin et al., 2022), except in parasitic Viscaceae (Petersen et al., 2015).

Pogoniopsis, a mycoheterotrophic orchid genus endemic to Brazil, represents one of the estimated ~50 losses of photosynthesis in fully mycoheterotrophic land plants. It comprises two species, *Pogoniopsis schenckii* and *P. nidus-avis*. The former is a perennial species endemic to the Brazilian Atlantic forest, where it is found in the forest understory. As is the case in many mycoheterotrophic plants (e.g., Merckx and Freudenstein, 2010; Merckx et al., 2013; Tsukaya, 2018), *P. schenckii* displays extremely reduced vegetative morphology. The only visible aboveground structure is the inflorescence during the flowering period, which has conspicuous flowers (Alves et al., 2021). The species is at least partially selfing, and seeds germinate while still inside fruit after the inflorescence falls into the leaf litter (Alves et al., 2021). There is extreme reduction in the ovule integuments (i.e., completely ategmic ovules lacking a micropyle), which has not been observed in other orchids (Alves et al., 2019) and is otherwise very rare in angiosperms (Bouman, 1984; Brown et al., 2010; Sato and Gonzales, 2017). This structural reduction does not appear to compromise its ability to produce seeds, as the synergids continue to secrete substances for pollen-tube attraction, penetration, and subsequent fertilization (Alves et al., 2019). Endophytic fungal hyphae are found in its aboveground and belowground organs, and may even reach the seeds by penetrating developing fruits (Alves et al., 2019, 2021). In addition, non-mycorrhizal endophytic fungi have been isolated from fruits and roots of *P. schenckii* that participate in seed germination, suggesting a possible symbiotic association throughout their life cycle (Sisti et al., 2019; Alves et al., 2021).

However, confirmation of the identity of the soil-fungal partners that must provide carbon and other nutrients to *Pogoniopsis* species is needed.

The extensive morphological modifications observed in *Pogoniopsis* mirror its uncertain placement in Orchidaceae phylogeny (see the recent review of systematic treatments in Cameron and van den Berg, 2017). The genus was initially described as having affinities with *Pogonia* (Reichenbach, 1881), and was placed in tribe Pogonieae (subfamily Vanilloideae) along with *Pogonia*, *Cleistes*, and *Psilochilus* (Martius et al., 1893). However, while addressing the possible placement of *Pogoniopsis* in tribe Pogonieae, Cameron (2003) noted that its current position is dubious, and indicated that it may instead be related to *Triphora* (Epidendroideae) based on several reproductive features (e.g., possession of tetrasporangiate anthers: Freudenstein and Rasmussen, 1999; Alves et al., 2021). This purported relationship is consistent with a phylogenetic study based on one nuclear (18S rDNA) and two mitochondrial (*atp*A, *nad*1b-c) regions (Cameron and van den Berg, 2017). The latter parsimony-based placement also aligns with its South and Central American distribution, as with other members of Triphoreae (Cameron, 2003). More recent taxonomic revisions have therefore placed *Pogoniopsis* in tribe Triphoreae (Epidendroideae) (Chase et al., 2015). However, its local position with respect to tribe Triphoreae and multiple other clades in Epidendroideae was poorly supported in the phylogenetic study of Cameron and van den Berg (2017). In the meantime, other publications have continued to consider *Pogoniopsis* as a member of subfamily Vanilloideae based on various data types, including nuclear markers (Pansarin et al., 2008, 2012) and fruit morphology (Pansarin, 2016, 2021). This continuing uncertainty points to a need for further study of its phylogenetic relationships.

Here, we recovered plastid and mitochondrial data sets from *P. schenckii* to more accurately place this fully mycoheterotrophic lineage in orchid phylogeny, and to document the effects of the gain of heterotrophy in this genus on plastid genome structure, evolution, and function. Full mycoheterotrophy in *P. schenckii*, with associated loss of photosynthesis, is thought to have evolved independently of the other heterotrophic lineages with sequenced plastid genomes, and thus represents a novel "evolutionary experiment" in what it means to be a heterotrophic plant. We use various lines of phylogenomic evidence to address the following questions: (1) Do plastid and mitochondrial phylogenomic data allow us to infer a robust placement of *P. schenckii* in orchid phylogeny? (2) What plastid genome structural changes (e.g., genome rearrangements, gene and intron loss) occurred following this independent origin of mycoheterotrophy? (3) What changes in selection occurred in retained plastid genes that may reflect the shift from an autotrophic to a heterotrophic lifestyle?

MATERIALS AND METHODS

Sequencing and assembly

We generated an Illumina Nextera-based genomic library (Illumina, San Diego, California, USA) of *Pogoniopsis schenckii* from genomic DNA obtained using the method of Doyle and Doyle (1990). This was sequenced as 100 bp paired-end reads on an Illumina HiSeq. 2000, in a multiplexed lane with nine other libraries. The resulting raw reads were demultiplexed and trimmed using CASAVA version 1.8.2 (Illumina), and we assembled a complete plastid genome de novo, based on two parallel approaches. First, we used NOVOPlasty version 2.7.2 (Dierckxsens et al., 2017) with default settings except for setting genome size from 10 to 200 kb, 101 bp read length, and 400 bp insert size. The plastid *acc*D locus (*Vanilla planifolia*, Orchidaceae, Asparagales; MN200375.1) served as a seed for assembly, which yielded a single 14,015 bp contig. We also generated assemblies in CLC Genomics Workbench version 6.5.1 (CLC bio, Aarhus, Denmark) with default settings, selecting all contigs >500 bp long and >30X coverage, and conducted local BLASTn- and BLASTx-based searches (Wheeler et al., 2003) using *Vanilla planifolia* plastid protein-coding genes as queries to identify contigs of putative plastid origin. This resulted in three large (>1500 bp) assemblies. We then used local BLAST searches with a set of protein-coding mitochondrial genes from *Allium cepa* (Amaryllidaceae, Asparagales; NC030100.1) as queries, to check that the CLC-based assemblies do not represent cryptic mitochondrial inserts of plastid genes (e.g., Fejes et al., 1988; Petersen et al., 2019; Shtratnikova et al., 2020); we did not uncover potential inserts, and plastid origin is also supported by their having higher average copy number than the corresponding mitochondrial contigs (i.e., 611.6X vs. 15.82X; and see below). We may have recovered the three separate contigs because CLC appears to struggle to assemble across the plastid IR boundaries; we connected the contigs with Sequencher version 4.8 (Gene Codes, Ann Arbor, Michigan, USA) using default settings. We also designed primers with Primer3 (Koressaar and Remm, 2007; Untergasser et al., 2007) (Appendix S1) to verify contig overlap using Sanger sequencing. To do this we amplified targets using Phusion High Fidelity DNA Polymerase (Thermo Fisher Scientific, Waltham, Massachusetts, USA) and sequenced them using BigDye Terminator version 3.1 sequencing chemistry (Applied Biosystems, Foster City, California, USA) on an Applied Biosystems 3730 S 48-capillary DNA Analyzer (Thermo Fisher Scientific) platform, using amplification primers for sequencing in both directions. Amplification and sequencing methods are as described in Lam et al. (2015). The compiled CLC contigs produced the same 14,015 bp genome that NOVOPlasty assembled.

We annotated the plastid genome assemblies using GeSeq (Tillich et al., 2017), employing the most sensitive settings (25% protein ID, 25% RNA ID) to identify initial

gene sequences, which we compared to the plastid genes of *Vanilla planifolia* (MN200375.1) to infer start and end positions for protein-coding genes. In order to identify cryptic/highly diverged plastid genes, we used NCBI OrfFinder (Wheeler et al., 2003) to characterize all non-nested open reading frames (ORFs) longer than 75 nucleotides that start with ATG (or that are potentially consistent with this start site, assuming RNA editing). We examined these ORFs with local BLASTx (Wheeler et al., 2003) to pull out the subset with significant hits to the protein-coding genes of *Vanilla planifolia*, using an E-value upper cutoff of 0.01. We then used cmscan in Infernal version 1.1.2 (Nawrocki and Eddy, 2013), with default parameters, to identify and annotate plastid rDNA and tRNA genes, based on calibrated models downloaded from Rfam.org for the bacterial 5S rDNA, 23S rDNA, and 16S rDNA genes. We also constructed alignments of putative *Pogoniopsis* tRNA sequences with corresponding genes from 13 complete plastid genomes from other orchids (see Appendix S2), converted into a searchable HMM profile using the hmmer version 3.3.2 tool suite (Eddy, 1998). We compared the set of rDNAs and tRNA genes retrieved using this method to those annotated in other orchids, in order to verify gene boundaries, and used VARNA version 3.93 (Darty et al., 2009) to draw the minimum free-energy secondary structure of *trn*E according to the orientation of the molecule in Su et al. (2019). Finally, we used OGDraw (Greiner et al., 2019) to generate the plastome map, represented in circular form for convenience.

For the mitochondrial gene assembly, we filtered contigs assembled by CLC for those >200 bp and with sequence depth >10X and then used BLASTn with a database of mitochondrial genes from *Sobralia macrantha* from Li et al. (2019) as query sequences; this approach identified 32 protein-coding genes in *Pogoniopsis* with hits to mitochondrial genes. The recovered set omits several short genes (*atp*4, *atp*9, *ccm*b, *rpl*5, *rps*1, and *rps*13), compared to the ~38 genes typical of angiosperm mitochondrial genomes. Mitochondrial gene number in angiosperms typically varies by around one to six genes (Knoop, 2004; Li et al., 2009). The unrecovered genes here may reflect either comparable gene losses or failure to recover genes that are still present. The latter possibility may be more likely, given the relatively low coverage of mitochondrial data here, and needs further investigation. We did not attempt to assemble full mitochondrial genomes, because they evolve very rapidly at the structural level (e.g., Kozik et al., 2019).

Alignment

For the plastid matrix, we compiled individual alignments for 76 protein-coding plastid genes (excluding *ycf*1 and *ycf*2 due to alignment difficulties) for *Pogoniopsis* and 60 orchid species that represent a broad array of autotrophic orchid genera, with one terminal for each included genus, and a broad array of monocot outgroup taxa (Appendix S2). The orchid sequences came from plastid gene matrices in Li et al. (2019), Givnish et al. (2015), Serna-Sánchez et al. (2021), and GenBank; we included genomes from taxa in each genus that have the most complete recovered genes. The selected orchid taxa represent all five subfamilies, and 19 of 22 tribes recognized by Chase et al. (2015). We added the orchids to a larger matrix comprising 214 autotrophic monocot taxa from Lam et al. (2018), which represents all 12 orders recognized by Givnish et al. (2018), yielding a total of 275 taxa. We aligned each gene using "alignSequences" in MACSE version 2 (Ranwez et al., 2018), with default parameters; this method attempts to preserve complete codons during automated alignment (codon-agnostic algorithms like MUSCLE and MAFFT can potentially be misled by the AT-rich genes of highly reduced mycoheterotroph plastomes). We further adjusted alignments manually in AliView version 1.27 (Larsson, 2014), considering criteria in Graham et al. (2000), and staggered several difficult-to-align regions (e.g., Steane et al., 1999; Graham et al., 2006; Bell et al., 2020). Missing genes were coded as missing data. We used a custom Python script (https://github.com/nklimpert/Pogoniopsis_phylogenetics) to concatenate the individual gene alignments into a single 87,648 bp matrix. We also translated the concatenated matrix into a 29,216-residue amino acid matrix using AliView (Larsson, 2014).

For the mitochondrial matrix, we assembled 38 individual gene matrices with 68 other taxa from Li et al. (2019). We aligned each mitochondrial gene matrix using MAFFT version 7.487 (Katoh, 2013), with inspection and manual adjustments done in AliView (Larsson, 2014); we found MACSE to be unnecessary for the mitochondrial alignments, likely due to their lower substitution rates and AT content. In situations where the mitochondrial genes were incomplete in *P. schenckii*, we aligned the recovered gene fragments to full mitochondrial genes from *Sobralia macrantha*, and coded gaps as missing data. We then used the custom Python script to concatenate the gene alignments, resulting in a 35,658 bp nucleotide matrix and a translated 11,886-residue amino acid matrix.

Phylogenetic inference

We performed phylogenetic analyses using unpartitioned and partitioned likelihood models for DNA and amino acid matrices. The initial schemes for DNA data partitioned the matrices by gene and codon position ("G × C"; e.g., Lam et al., 2015; Soto Gomez et al., 2020), representing 222 partitions for plastid DNA matrix and 114 partitions for the mitochondrial DNA matrix. We treated each gene in the amino acid (AA) matrices as individual data partitions, corresponding to 76 initial partitions for the plastid data (12 for *P. schenckii*, with the rest coded as missing data) and 38 initial partitions for the mitochondrial data (32 for *P. schenckii*, with the rest as missing data for this taxon). We then used IQ-TREE version 2.1.2 (Nguyen et al., 2015) on the CIPRES Science Gateway (Miller et al., 2010) to merge

partitions with similar substitution models, estimating best-fit substitution models for each partition using the "TESTMERGEONLY" option. The optimal partitioning schemes and substitution models were selected using the Bayesian Information Criterion (BIC; Watanabe, 2013). In several cases where the optimal substitution model for a partition was not implemented in RAxML-NG, we employed a close alternative model (Appendix S3). We also used IQ-TREE to select best-fit substitution models for the unpartitioned versions of the DNA and amino-acid alignments.

Overall, we performed four phylogenetic analyses on the plastome data and four on the mitochondrial data (i.e., for each genome, unpartitioned and partitioned analyses of the respective DNA and AA matrices). The tree searches were executed using RAxML-NG version 1.0.0 (Kozlov et al., 2019) on the CIPRES server (Miller et al., 2010). Our two concatenated matrices have a high number of parsimony-informative sites (28,873 parsimony informative sites total for the plastid matrix, 3255 parsimony informative sites across the mitochondrial matrix), which should make them much less prone than corresponding inferences based on single genes to non-reproducibility concerns raised by Shen et al. (2020) for RAxML-NG and other heuristic inference methods. We searched for the best likelihood tree in each case using 10 random starting trees and 10 parsimony-based starting trees, for a total of 20 replicates per analysis. We also assessed branch support by bootstrap analysis using thorough searches ("full bootstrapping") and 500 bootstrap replicates (Felsenstein, 1985). The analyses were also repeated on partitioned DNA matrices of plastid and mitochondrial data sets with *P. schenckii* removed, to assess whether its inclusion tends to depress bootstrap support near its point of attachment in the inferred tree. In this case, we removed gaps in the matrices left by the exclusion of *P. schenckii*, and again used IQ-TREE to find the optimal partitioning schemes and models for each matrix before performing searches.

Characterizing genome rearrangement

We used Mauve (Darling et al., 2004; version 20150226, build 10) to assess changes in gene order in the plastid genome of *P. schenckii*, using the ProgressiveMauve option with default settings. Mauve determines conserved homologous regions (locally colinear blocks, or LCBs) between sequences and positions them with a progressive alignment algorithm. We compared the plastid genome of *P. schenckii* to five species (*Apostasia wallichii*, *Vanilla pompona*, *Paphiopedilum micranthum*, *Anoectochilus emeiensis*, and *Cymbidium aloifolium*) representing each of the Orchidaceae subfamilies. We chose a consistent starting point for each sequence and removed one copy of the inverted repeat to facilitate the analysis. We also arranged the small single-copy region (SSC) to have a consistent orientation in all six sequences (the SSC is found as both inversion isoforms in equimolar ratios; Palmer, 1985).

Tests for change in selective regime

We conducted a test for changes in the strength of selection acting on plastid genes using the CodeML module in PAML version 4.9 h (Yang, 2007), conducting a branch test (Yang, 1998) for each protein-coding gene, using a 30-taxon subset (Appendix S2) of the complete matrix. This test assesses whether there is a significant difference in the average dN/dS (the ratio of nonsynonymous substitutions per nonsynonymous site to synonymous substitutions per synonymous site, also referred to as ω) for a gene along a given branch in a tree (i.e., the assigned foreground branch vs. the background branches). We used the topology inferred by the ML analysis on the partitioned plastid DNA data. In practice the tests performed here detect increases or decreases in the strength of purifying selection, as the ω-values were all <1.0 (see below). For these tests, we used trimAl version 1.2rev59 (Capella-Gutiérrez et al., 2009) to remove any aligned regions with data missing for ≥90% of the included taxa, and used a likelihood ratio test to compare the test models to the null models, calculating the significance of model differences between *P. schenckii* and its autotrophic relatives based on a chi-square test with a single degree of freedom, with a Benjamini-Hochberg correction for multiple tests across genes.

We also tested for relaxation of selective pressure on plastid genes using RELAX version 2.1 (Wertheim et al., 2015) as implemented in HyPhy version 2.3.14 (Kosakovsky Pond et al., 2005). Rather than estimating dN/dS directly, RELAX estimates whether the selection on a gene has experienced relaxed or intensified selection along a branch. Although RELAX is unable to differentiate between changes in purifying selection vs. positive selection, a k-value closer to 1.0 (neutral evolution) in the foreground compared to the background indicates relaxed selection; values further from 1.0 suggest intensified selection. We used custom shell scripts (https://github.com/nklimpert/Pogoniopsis_phylogenetics) to run individual RELAX analyses with the same reduced gene matrices used for the PAML analyses.

RESULTS

Plastid genome

We assembled a complete 14,015 bp plastid genome for *Pogoniopsis schenckii* (presented in a circular form in Figure 1). This assembly includes 101,179 reads and has an average 611.6X coverage. It comprises two single-copy regions of similar length (5276 bp and 5721 bp, with the slightly larger region corresponding approximately to the LSC of most plastid genomes), separated by short inverted repeats (IRs) (1509 bp each). The GC content of the plastome is 23.94%, with only 20.64% average GC content for the protein-coding genes. We recovered 12 protein-coding genes for *Pogoniopsis*, all of which are included in

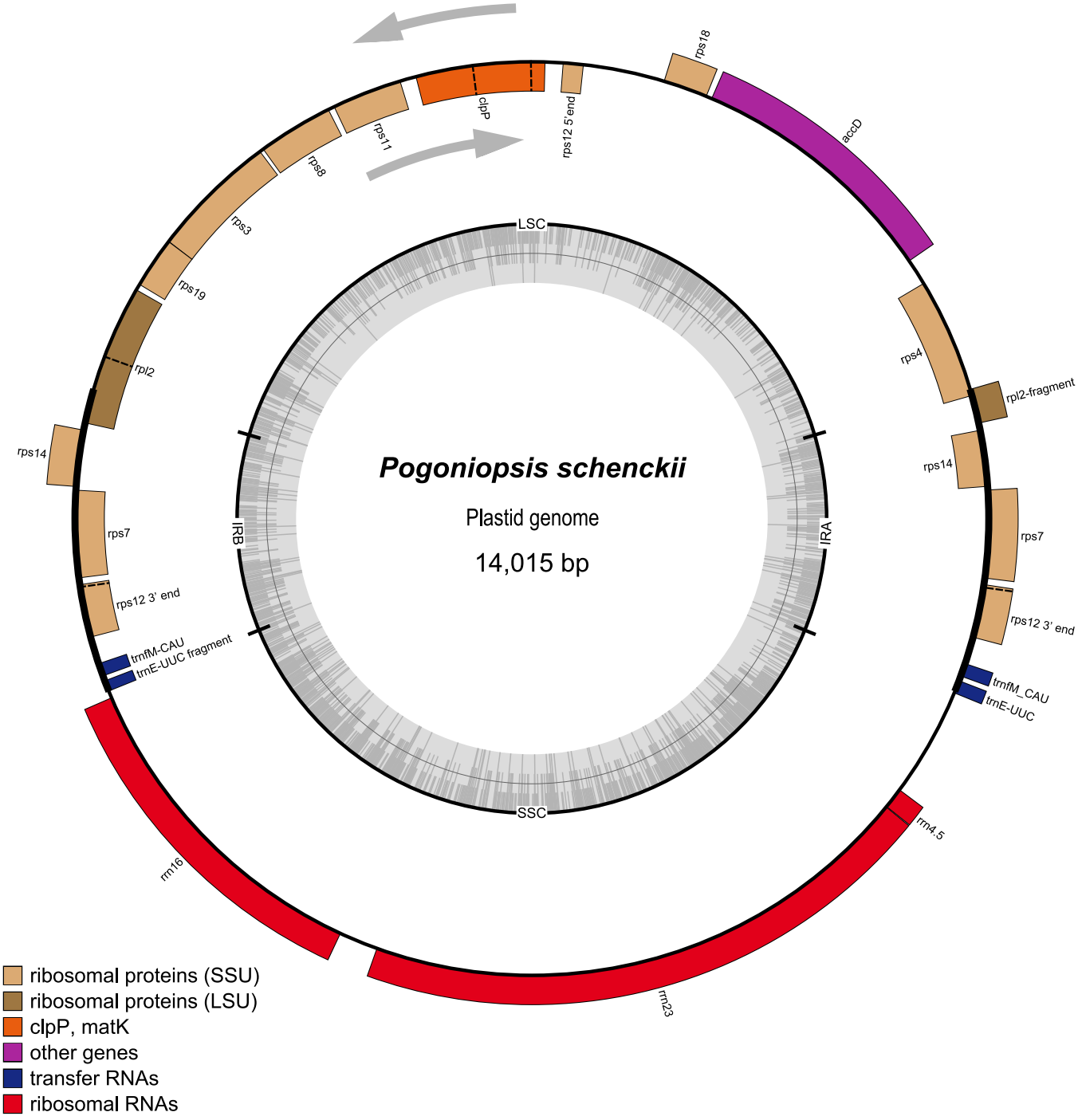

FIGURE 1 Full plastid genome of *Pogoniopsis schenckii*, represented as a circle. Major functional classes of retained genes are indicated (see key); the inverted repeat region and small and large single-copy regions are marked (as IR_A/IR_B, SSC, LSC, respectively). Dashed lines in several genes indicate intron deletions in comparison to other plants. Gray arrows indicate direction of transcription. Gray bars in central circle depict average GC content across a 20 bp sliding window.

phylogenetic inference (see below). Ten of these code for translational apparatus subunits (i.e., *rpl*2, *rps*3, *rps*4, *rps*7, *rps*8, *rps*11, *rps*12, *rps*14, *rps*18, and *rps*19); *acc*D and *clp*P code for subunits of acetyl-coA carboxylase and Clp-protease, respectively (Table 1). All twelve of the retained protein-coding genes have intact reading frames. The retained plastid genes have lost all *cis*-spliced introns present in most other angiosperms (normally present in *rpl*2, *rps*12, and *clp*P). However, *trans*-splicing of two exons of *rps*12 is likely still required, assuming this protein is still functional. In addition, we recovered three rDNA loci (*rrn*4.5, *rrn*16, and *rrn*23) and two tRNA sequences (*trn*E-UUC and *trn*fM-CAU; Table 1). We did not recover a 5S rDNA locus (*rrn*5S). Both retained tRNA sequences are

TABLE 1 Genes recovered from the *Pogoniopsis schenckii* plastid genome vs. those typically present in autotrophic angiosperms. Asterisks indicate genes that typically have *cis*-spliced introns but are intron-free here; of these, *rpl*2 and 3′-*rps*12 usually each contain a single group IIA intron, and *clp*P usually contains a group IIA and a group IIB intron. Genes missing in *Pogoniopsis* that contain *cis*-spliced introns in most other angiosperms are (1) *atp*F, *trn*A-UGC, *trnI*-GAU, *trnK*-UUU, and *trnV*-UAC (all group IIA introns); (2) *ndh*A, *ndh*B, *rpl*16, *rpo*C1, *rps*16, *pet*B, *pet*D, *trn*G-UCC, and *ycf3* (introns 1 and 2) (all group IIB introns); and (3) *trn*L-UAA (a group I intron).

Function	Gene names	Number retained (of total)[a]
Photosynthesis	–	0 (48)
Translational apparatus	*rpl*2*, *rps*3, *rps*4, *rps*7, *rps*8, *rps*11, 3′-*rps*12*, *rps*14, *rps*18, *rps*19	10 (22)
Plastid-encoded RNA polymerase	–	0 (4)
rDNA loci	*rrn*4.5, *rrn*16, *rrn*23	3 (4)
tRNA loci	*trnf*M, *trn*E	2 (29)
Other protein-coding genes	*acc*D, *clp*P*	2 (5)

[a]Based on Wicke et al. (2011).

predicted to have the canonical cloverleaf shape expected of functioning tRNAs (based on minimum free energy structural predictions), although *trn*E-UUC has lost its UUC anticodon sequence (Figure 2).

Apart from the incorporation of *trn*E-UUC and *trnf*M-CAU into the IR, gene order in the *P. schenckii* plastome is nearly colinear with the plastomes of autotrophic orchids (Figure 3; Appendix S4). The *Pogoniopsis* IRs include genes found in IRs of other orchids (e.g., those shown for *Cymbidium aloifolium* in Figure 3), setting aside several that have been lost from the plastome (i.e., *rpl*22, *ycf*2, and *ndh*B). However, the boundaries of the IRs have shifted to exclude *rps*3, *rps*19, part of *rpl*2 (all now in the LSC), and *rrn*16, *rrn*23, and *rrn*4.5 (the only complete genes now found in the SSC; Figure 1).

Inference of phylogenetic placement of *Pogoniopsis* in orchid phylogeny

All eight analyses of plastid and mitochondrial data place *Pogoniopsis schenckii* in subfamily Epidendroideae (summarized in Table 2; see Figures 4–6; Appendices S5–S12). Two of the inferred placements within Epidendroideae have ≥90% bootstrap support (i.e., the unpartitioned and partitioned mitochondrial DNA analyses; Table 2; Figure 5; Appendices S9, S10). Most analyses only place it with weak supported at the tribal level, in variant positions across analyses (summarized in Table 2; Appendices S5–S8, S11–S12). Only two analyses place it with moderately strong bootstrap support—once again the unpartitioned and partitioned mitochondrial DNA analyses, which both place it near tribe Sobralieae as sister to *Sobralia macrantha* among sampled taxa (73% and 77% bootstrap support, respectively; see also Figure 5; Appendices S9, S10). Some of the uncertainty in its placement in a subset of analyses may reflect the highly elevated substitutional rates of *Pogoniopsis*, which is much more extreme for plastid than mitochondrial data (see summary phylogram for the DNA analyses in Figure 6). *Pogoniopsis* rate elevation may also account for the observed local depression in bootstrap support around its point of attachment to orchid phylogeny (for example, compare when *Pogoniopsis* is included vs. excluded from analyses; branches with reduced support for the former vs. latter case have circled values in Figures 4 and 5). This apparently depressive effect appears to be much more extreme in plastid than in mitochondrial analyses (cf. Figures 4 and 5), with only two branches affected near the point of attachment of *Pogoniopsis* in the latter case, and then only with mild depression in bootstrap support (~15% for both affected branches in the mitochondrial tree; Figure 5).

Both plastid and mitochondrial analyses otherwise agree broadly on relationships in Orchidaceae (Figures 4 and 5; Appendices S5–S12). Setting aside the position of *Pogoniopsis*, all recognized subfamilies and tribes of orchids are inferred to be monophyletic across all analyses. The most significant difference among analyses concerns the relative order of subfamilies Cypripedioideae and Vanilloideae and related subfamilies. In plastid analyses, Vanilloideae are inferred to be the sister group of the following clade with 52%–85% bootstrap support across analyses (Cypripedioideae, (Orchidoideae, Epidendroideae)) (Figure 4; Appendices S5–S8); in contrast, the mitochondrial analyses place Cypripedioideae as sister to (Vanilloideae, (Orchidoideae, Epidendroideae)), with 93%–100% bootstrap support for the relevant branches (Figure 5; Appendices S9–S12).

Changes in selective regime in retained plastid genes of *Pogoniopsis*

Branch tests of selection on the twelve retained protein-coding genes all indicate purifying selection ($0.080 < \omega < 0.453$;

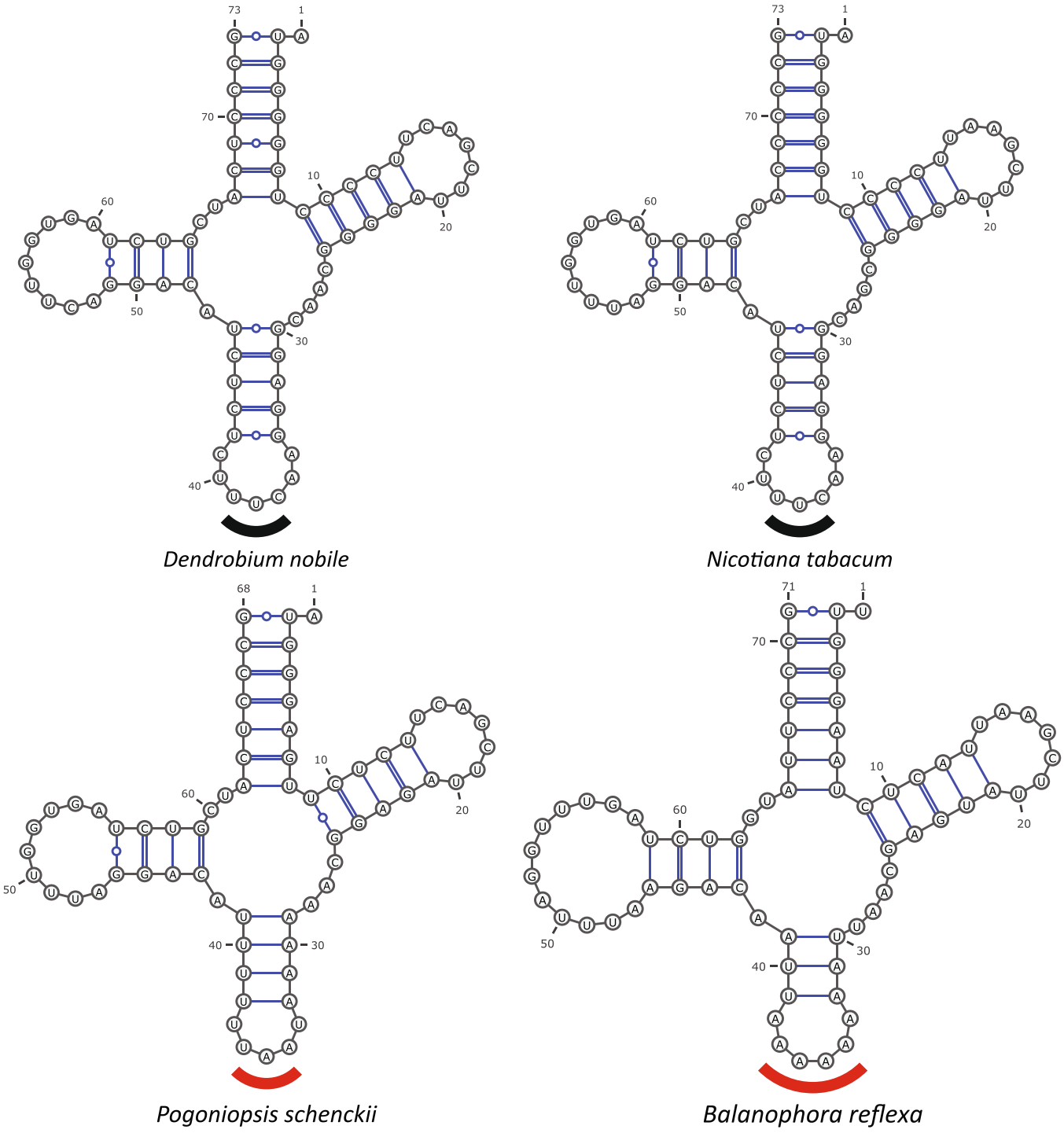

FIGURE 2 Predicted "cloverleaf" secondary structure of plastid *trn*E-UUC for two autotrophic angiosperms (black font: *Nicotiana tabacum*, Solanaceae; *Dendrobium nobile*, Orchidaceae) and two heterotrophic taxa with disrupted anticodons (*Pogoniopsis schenckii*, Orchidaceae; *Balanophora reflexa*, Balanophoraceae). Anticodons are indicated with a thick black line for autotrophic taxa; thick red lines indicate corresponding regions in heterotrophic taxa.

Table 3A, Figure 7A), even though both synonymous and nonsynonymous substitution rates are massively elevated in the genes of *Pogoniopsis*. However, the *d*N/*d*S ratio is significantly different between *Pogoniopsis* and its autotrophic relatives for only two genes, *acc*D and *rpl*2 (0.080 vs. 0.411 and 0.103 vs. 0.253, respectively; $P < 0.005$ after Benjamini-Hochberg corrections; Table 3A, Figure 7A). This implies a strengthening of purifying selection in *Pogoniopsis* for these two genes. In contrast, the RELAX tests indicated significant intensification of selection only for *acc*D (Table 3B, Figure 7B).

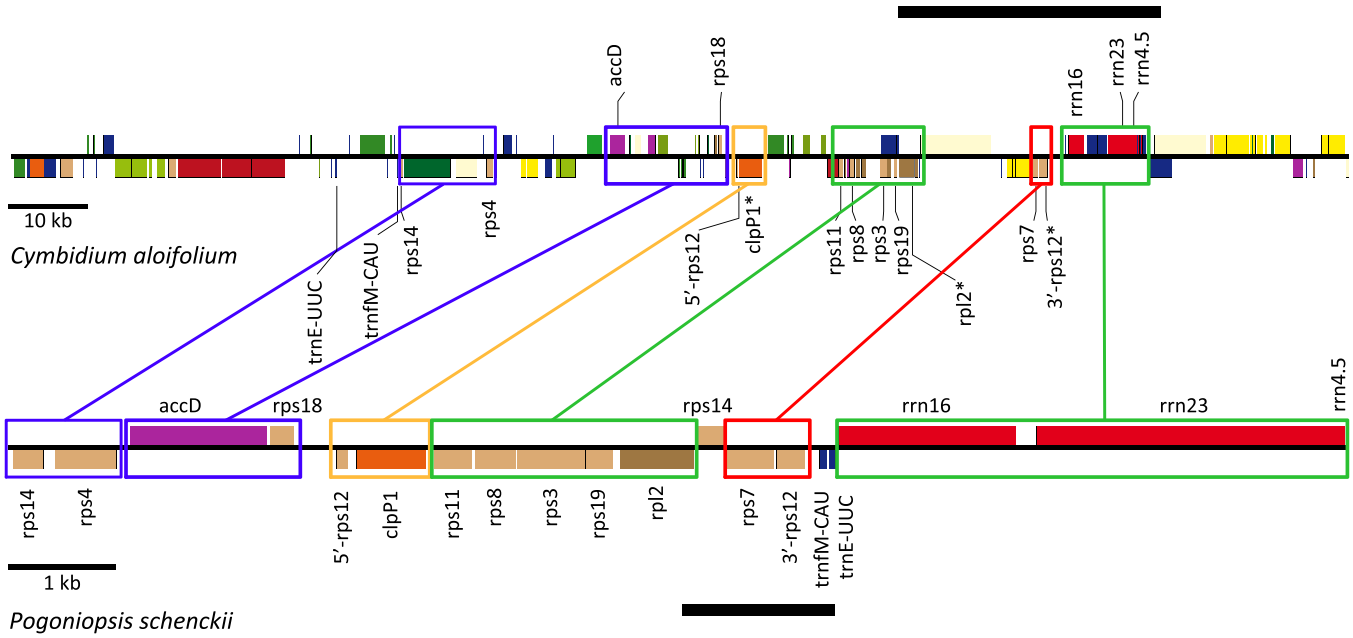

FIGURE 3 Comparison of gene order in the plastid genomes of *Pogoniopsis schenckii* and *Cymbidium aloifolium* (one copy of the inverted repeat removed in each case). The linearized maps of the two plastid genomes show relative gene orders; colored boxes connected by lines indicate groups of orthologous genes in the same order. Scale bars are indicated below each plastid genome. Thick black bars above *Cymbidium* and below *Pogoniopsis* indicate relative positions of the inverted repeat, with the large single-copy region to the left and small single-copy region to the right. Asterisks indicate intronless genes in *Pogoniopsis* that have introns in *Cymbidium*.

TABLE 2 Inferred placements of *Pogoniopsis schenckii* based on various analyses of plastid and mitochondrial data considering DNA or amino acid (AA) data. Placements to subfamily and tribe are indicated, along with associated bootstrap support values for the clade as a whole (see Figures 4 and 5; Appendices S5–S12).

Organelle	Type of data	Likelihood method	Local placement of *P. schenckii* in/near subfamily (tribe)	Support for local in subfamily/tribe
Plastid	DNA	Unpartitioned	Epidendroideae (Vandeae)	39/13
		Partitioned	Epidendroideae (Vandeae)	55/20
	AA	Unpartitioned	Epidendroideae (Vandeae)	70/27
		Partitioned	Epidendroideae (Vandeae)	70/26
Mitochondrial	DNA	Unpartitioned	Epidendroideae (Sobralieae)	91/73
		Partitioned	Epidendroideae (Sobralieae)	99/77
	AA	Unpartitioned	Epidendroideae (Tropidieae)	64/42
		Partitioned	Epidendroideae (Tropidieae)	63/42

DISCUSSION

Improved understanding of the placement of *Pogoniopsis* in orchid phylogeny

Plastid and mitochondrial genomes consistently place *Pogoniopsis* within subfamily Epidendroideae, with poor to moderate support here for plastid data (based on unpartitioned vs. partitioned DNA analyses), moderate support from the plastid amino-acid analyses (Table 2, Figure 4; Appendices S5–S8), and poor to strong support for the mitochondrial data (poor for amino acid analyses, and moderate to strong for DNA analyses: Table 2, Figure 5; Appendices S9–S12). This general result agrees with the findings of Cameron and van den Berg (2017) based on their small (three gene) data set, but is inferred here with generally stronger support. Our placement of *Pogoniopsis* in Epidendroideae also aligns with floral morphological features shared by *Pogoniopsis* and other Epidendroideae, as pointed out by Cameron (2003) and Chase et al. (2015), including details of the column structure and anther position.

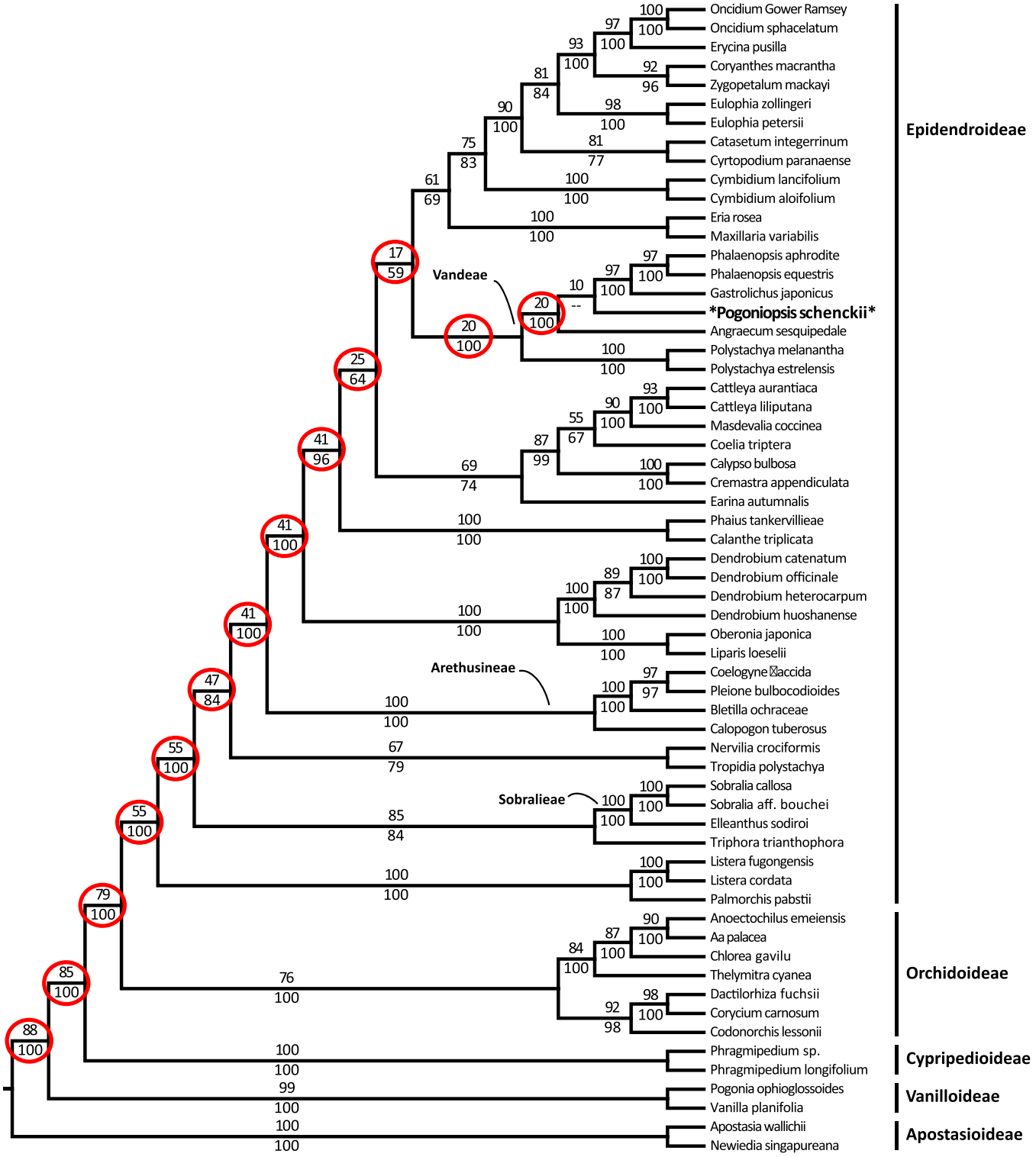

FIGURE 4 Plastid-based placement of *Pogoniopsis schenckii* in Orchidaceae based on analysis of 76 protein-coding genes (only 12 genes for *Pogoniopsis*) using partitioned likelihood analysis of the DNA data set for this organelle (for full analysis, see Appendix S6). Numbers above vs. below branches represent bootstrap support values with *Pogoniopsis* included vs. excluded from consideration (circled values are depressed by ≥10% when *Pogoniopsis* is included).

Although plastid data have been successfully used to infer placement of many heterotrophic plant species, several exceptions have been characterized for extremely rapidly evolving (rate-elevated) orchid lineages (e.g., *Epipogium* and *Rhizanthella*; Lam et al., 2018), consistent with expectations from theory that the most rapidly evolving lineages will be the most challenging to place (e.g., Felsenstein, 1978; Ho and Jermiin, 2004). In contrast, mitochondrial genomes

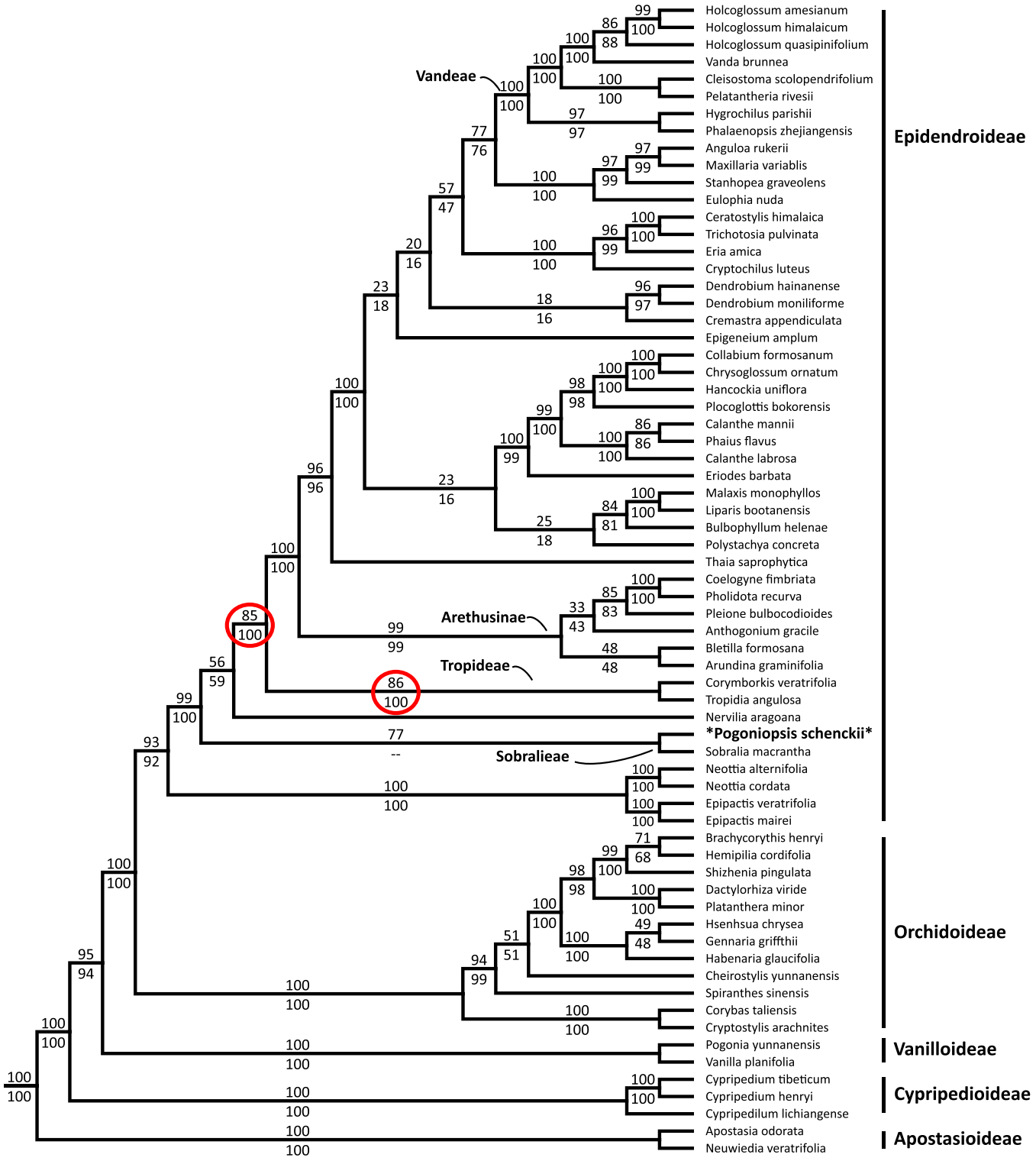

FIGURE 5 Mitochondrial-based placement of *Pogoniopsis schenckii* in Orchidaceae based on analysis of 38 genes (32 genes for *Pogoniopsis*) using partitioned likelihood analysis of the DNA data set for this organelle (for full analysis, see Appendix S10). Numbers above vs. below branches represent bootstrap support values with *Pogoniopsis* included vs. excluded from consideration (circled values are depressed by ≥10% when *Pogoniopsis* is included).

evolve more slowly in general (e.g., Wolfe et al., 1987; Palmer, 1990) and also display less elevated rates in heterotrophic lineages (e.g., Bromham et al., 2013; Petersen et al., 2019; Figure 6). This means that mitochondrial genomic data may be better suited to inferring the phylogenetic placement of heterotrophic lineages that have highly elevated plastid substitution rates, because of a reduced susceptibility of mitochondrial data to saturation/

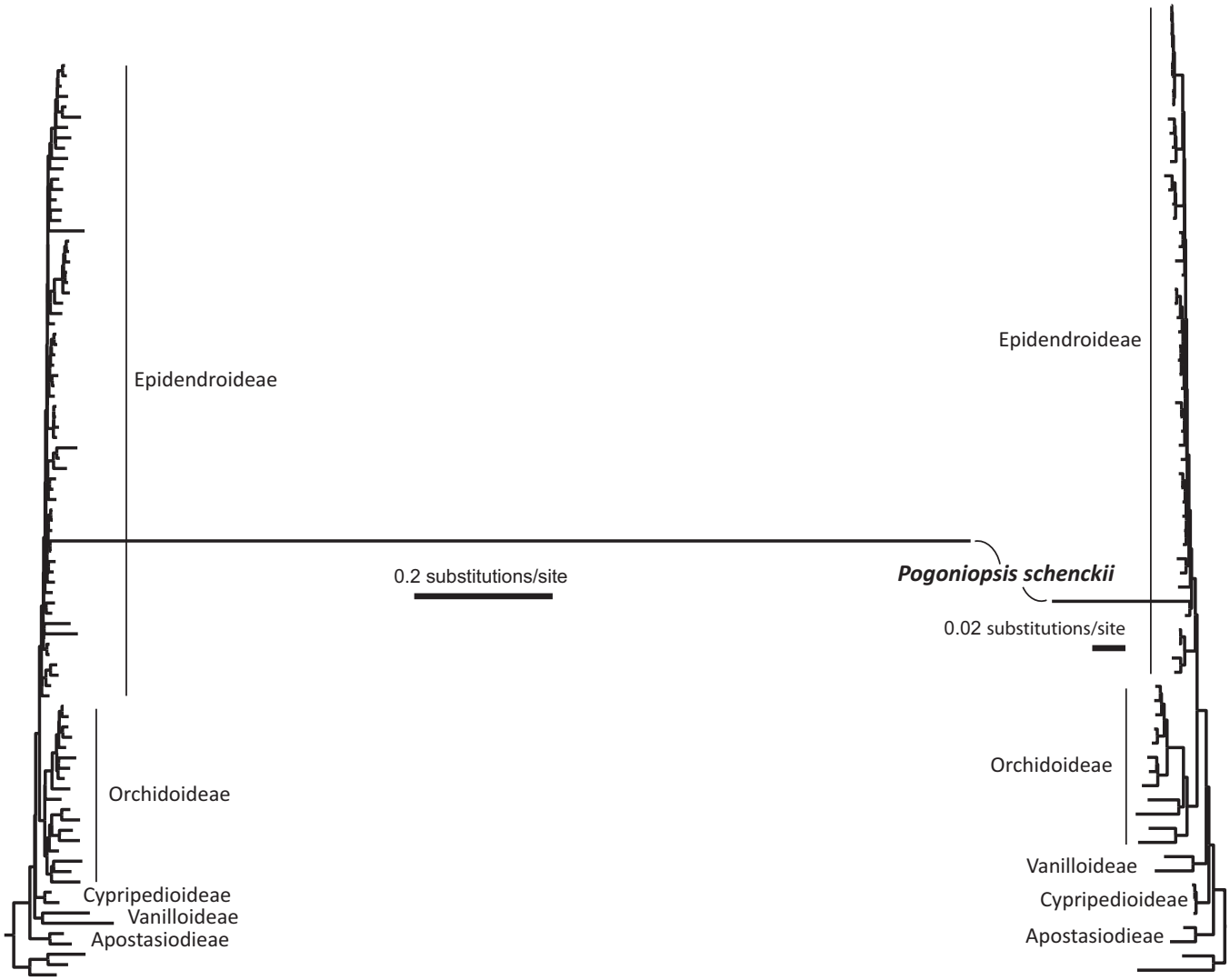

FIGURE 6 Likelihood-based phylograms of Orchidaceae summarizing rate elevation in *Pogoniopsis* in plastid vs. mitochondrial genomes for partitioned DNA likelihood analyses (for taxon names and support values, see Figures 4 and 5); scale bar shows the estimated number of substitutions per site.

long-branch attraction issues (Lin et al., 2022). The better performance of mitochondrial data here may also reflect fewer undiscovered instances of cryptically misaligned regions compared to plastid alignments. It is consistent with the mild and localized depression in branch support values observed here for the mitochondrial data, compared to the substantial and diffuse reductions in corresponding plastid analysis (cf. Figures 4 and 5). This may also explain several incongruent results between plastid and mitochondrial phylogenomic inferences that involve heterotrophic orchid lineages (Li et al., 2019).

Considering the mitochondrial phylogenomic data in more detail, our data provide moderate to strong support for the placement of *Pogoniopsis* at the tribal level (Table 2): all four mitochondrial analyses recover *P. schenckii* within a grade of terrestrial epidendroids (among the so-called "lower" epidendroids). In contrast, the tribal placement of *Pogoniopsis* is much less certain here in plastid-based inferences, which consistently place it in tribe Vandeae with poor support (Table 2; Appendices S5–S8). The mitochondrial data instead place it near tribe Sobralieae (DNA analyses: Figure 5; Appendices S9–S10) or Tropidieae (amino-acid analyses: Appendices S11–S12). Indeed, across all eight phylogenetic analyses here, only those based on mitochondrial DNA infer a tribal position of *Pogoniopsis* near Sobralieae with moderately strong support (Table 2). This result is consistent with morphology-based treatments (Cameron, 2003) and results based on nuclear ribosomal data (Cameron and van den Berg, 2017) that pointed to a position of *Pogoniopsis* in tribe Triphoreae, another "lower" epidendroid. The inference of relationships among these epidendroids may have been hampered by the relatively long branches that subtend the corresponding lineages (Freudenstein and Chase, 2015; Givnish et al., 2015). Although we were not able to obtain mitochondrial sequences for members of Triphoreae, future mitochondrial

TABLE 3 Tests of change in selective pressure in retained protein-coding genes of *Pogoniopsis schenckii* compared to autotrophic relatives ("auto"; see also Figure 7). (A) Branch-test analysis; ω-values are the ratio of synonymous and nonsynonymous substitution rates within each gene for *P. schenckii* and autotrophic relatives, (B) RELAX test results; *k*-values indicate intensification (>1.0) or relaxation (<1.0) of selection compared to autotrophic relatives. Asterisks indicate statistically significant results (after correction for multiple tests).

A. Branch tests

Gene	ω_{auto}	$\omega_{Pogoniopsis}$	Likelihood	*P*-value
*acc*D*	0.411	0.080	−7569.97	6.77E-13
*clp*P	0.194	0.101	−2726.22	0.025
*rpl2**	0.253	0.103	−2108.47	0.004
rps3	0.153	0.176	−3306.09	0.697
rps4	0.209	0.168	−2580.64	0.509
rps7	0.208	0.106	−1043.97	0.170
rps8	0.188	0.153	−1877.08	0.646
rps11	0.142	0.176	−2046.5	0.983
rps12	0.11	0.118	−950.902	0.607
rps14	0.267	0.309	−1338.05	0.878
rps18	0.243	0.453	−1237.96	0.723
rps19	0.148	0.149	−799.956	0.225

B. RELAX tests

Gene	*k*-value	*P*-value
accD*	3.373695	4.37E-07
clpP	1.211264	0.304393
rpl2	1.753669	0.030417
rps3	1.042859	0.850536
rps4	1.053584	0.939392
rps7	1.49656	0.271273
rps8	0.27363	0.022151
rps11	0.794757	0.411856
rps12	0.579123	0.184483
rps14	0.698371	0.412855
rps18	0.479692	0.232471
rps19	0.96333	0.89681

genomic sampling efforts should focus there, to place *Pogoniopsis* with even greater precision. The placement of *Pogoniopsis* and other rate-elevated heterotrophic orchids may also be addressed by building on recent nuclear phylogenomic data sets for Orchidaceae (Pérez-Escobar et al., 2021). However, the general extent of rate elevation across nuclear genes of heterotrophic plants and its impact on phylogenetic inference have not been well characterized to date (but see, e.g., Lemaire et al., 2011; Bromham et al., 2013).

Changes in selective regime in retained plastid genes of *Pogoniopsis*

In *P. schenckii*, all retained protein-coding genes appear to remain under strong purifying selection (ω « 1; Table 3A), consistent with studies of retained genes in other heterotrophic plants (e.g., Lam et al., 2015; Schelkunov et al., 2015; Joyce et al., 2018; Su et al., 2019; Yudina et al., 2021). Here, the branch-test analysis indicates that two genes (*acc*D and *rpl*2) in *P. schenckii* have experienced strengthening of purifying selection compared to their autotrophic relatives (Table 3A, Figure 7A). This is consistent with sporadic instances in other plastid genes of heterotrophs (e.g., Logacheva et al., 2011; Schelkunov et al., 2015; Roquet et al., 2016; Bell et al., 2020). The RELAX test also indicates intensified selection in *acc*D (Table 3B, Figure 7B). Caution should always be exercised when interpreting the results of these tests, as they can be sensitive to small errors in the sequence alignment in highly divergent taxa. Nonetheless, we took care to generate our alignments with manual inspection of machine-generated alignments. The observation for *acc*D, in particular, may have functional significance in *Pogoniopsis*, as *acc*D is involved in a non-photosynthetic plastid function (lipid biosynthesis) and has been observed to remain under purifying selection in other heterotrophic lineages (e.g., Lam et al., 2015; Schelkunov et al., 2015; Joyce et al., 2018; Su et al., 2019; Yudina et al., 2021).

Plastid genome structural evolution

Plastid genomes typically comprise ~78 protein-coding genes, 30 transfer RNA genes, and four rDNA genes (Palmer and Delwiche, 1998). The bulk of these genes (~40%) play a role in photosynthesis, but a major portion function as part of the plastid translational apparatus (Palmer and Delwiche, 1998; Wicke et al., 2011).

A cascade of gene loss in the plastomes of heterotrophic plants has been well characterized in multiple independent lineages of heterotrophic plants, with photosynthetic genes being the first to go, followed by those involved in the translational apparatus (e.g., Barrett and Davis, 2012; Barrett et al., 2014; Graham et al., 2017). Evidence from the sequenced nuclear genomes of other mycoheterotrophic species (e.g., *Gastrodia elata*: Yuan et al., 2018; *Gastrodia menghaiensis*: Jiang et al., 2022) indicates that the absence of photosynthetic genes in full heterotrophs represents complete loss, rather than representing functional transfer to the nucleus. Only a handful of genes have primary functions (*acc*D, *clp*P, *mat*K, *ycf*1, *ycf*2) or secondary functions (*atp* genes, *rbc*L, *trn*E) outside of photosynthesis or translation (e.g., Palmer and Delwiche, 1998; Barbrook et al., 2006; Wicke et al., 2011; Graham et al., 2017). Five genes with non-bioenergetic functions (*acc*D, *clp*P, *trn*E, *ycf*1, *ycf*2) are commonly observed to be among the last retained in drastically reduced plastid genomes (e.g., Barbrook

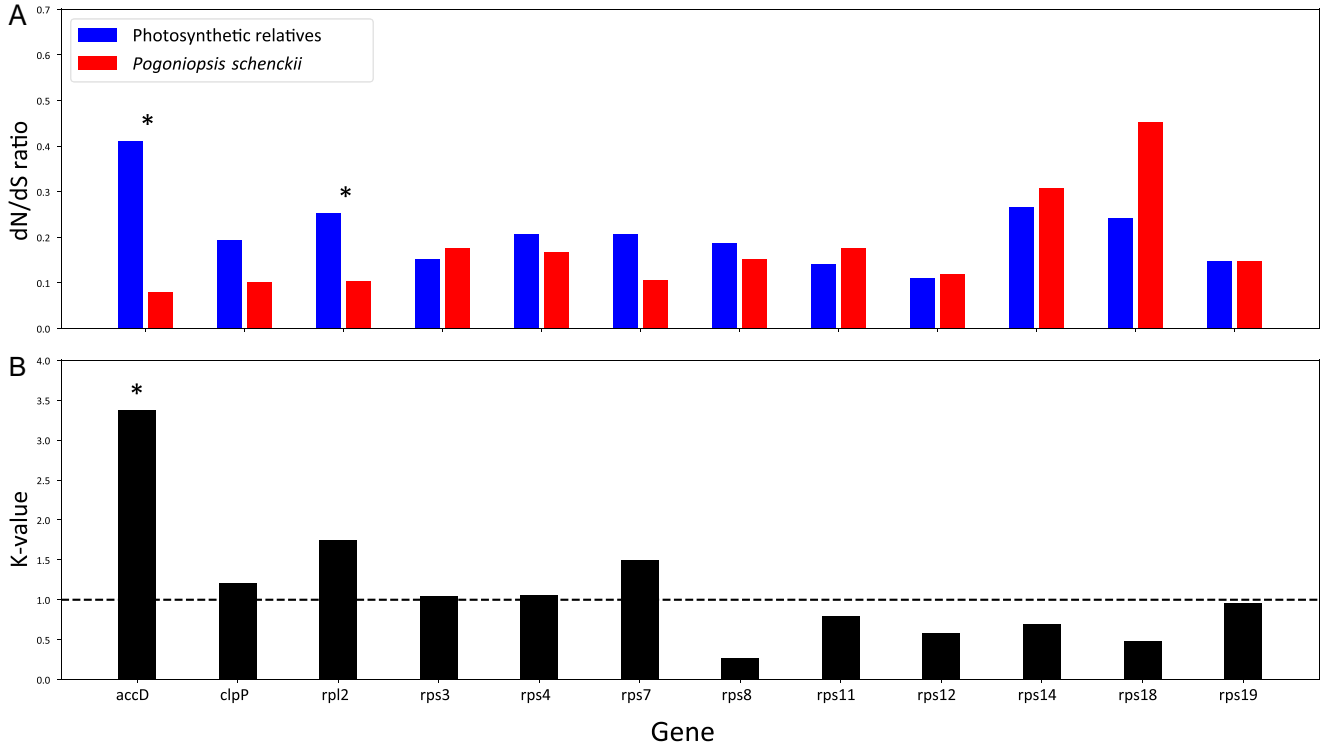

FIGURE 7 Tests for differences in selective pressure in retained protein-coding genes of *Pogoniopsis schenckii* compared to autotrophic relatives (subset noted in text; for more detail, see Table 3). (A) Summary of branch tests for individual retained genes. Bar heights are the ratio of nonsynonymous to synonymous (*d*N/*d*S) rates in *Pogoniopsis* (foreground taxon) or the background taxa; values <1.0 indicate purifying selection. (B) Summary of RELAX tests on changes in strength of selection in individual genes; *k*-values >1.0 indicate intensification of selection compared to autotrophic relatives. Asterisks indicate significant changes.

et al., 2006; Barrett and Davis, 2012; Barrett et al., 2014; Graham et al., 2017; Wicke and Naumann, 2018). *Pogoniopsis schenckii* fits with this general picture of extensive gene loss in full mycoheterotrophs (Table 1) and has also lost two of these five non-bioenergetic genes (*ycf*1, *ycf*2). Indeed, it possesses the smallest plastid genome recovered to date among orchids, and among the smallest among heterotrophic plants (e.g., Lam et al., 2018: app. S3; Yudina et al., 2021). It also ranks as among the smallest plastid genomes in terms of number of retained genes, with only 12 protein-coding genes, three rDNA genes, and two tRNA genes recovered (Table 1). This high level of loss is consistent with its being near a predicted end point of plastid genome reduction—the loss of the entire plastid genome, presumed to depend on the prior loss of all non-bioenergetic genes (e.g., Graham et al., 2017). In *Pogoniopsis* this would presumably require the loss of *acc*D, *trn*fM, *trn*E, and *clp*P from the plastid genome, all four of which have been lost individually in other lineages (e.g., Bellot and Renner, 2016; Naumann et al., 2016; Arias-Agudelo et al., 2019; Su et al., 2019; Jost et al., 2020; Liu et al., 2020; Ceriotti et al., 2021; Yudina et al., 2021).

However, despite its small size, the order of genes in the *Pogoniopsis* plastid genome is very similar to that of its autotrophic relatives (Figure 3; Appendix S4), with only small shifts in the IR boundaries. Specifically, the border with the LSC has shifted a few hundred base pairs inward to exclude most of the *rpl*2 gene. Thus, the IR of close autotrophic relatives includes a full copy of *rpl*2, but the IR in *P. schenckii* has contracted to include only a fragment of it (Figure 1). A larger contraction has occurred at the other IR border in *P. schenckii* to exclude the entirety of the *rrn*16–*rrn*23–*rrn*4.5 cistron. The latter region now comprises the bulk of the small single-copy region of its plastome (Figure 1). Small shifts in the IR boundaries are relatively common even among autotrophic lineages (e.g., Kim et al., 2015; Zhu et al., 2016; Lee et al., 2021), but in heterotrophic lineages whose plastid genomes retain IRs, shifts appear to be more common and larger in extent (e.g., Schelkunov et al., 2015; Joyce et al., 2018; Kim et al., 2019; Z. Li et al., 2020), consistent with what we found here. Nonetheless, the overall retention of colinearity in gene order in photosynthetic taxa is relatively unusual across heterotrophic lineages, as many reduced plastid genomes have also been observed to experience genome rearrangements (e.g., Lam et al., 2015; Schelkunov et al., 2015; Lim et al., 2016; Li et al., 2019; Yudina et al., 2021). This may be connected to the retention of the IR region, which has been hypothesized to play a role in plastid genome replication (e.g., Palmer and Thompson, 1982; Palmer, 1991; Mühlbauer et al., 2002; Scharff and Koop, 2007). The IR region has been lost in some autotrophic lineages, which

can coincide with increased genomic rearrangements (e.g., Palmer and Thompson, 1982; Zhu et al., 2016). However, not all mycoheterotrophic taxa lacking IRs have substantial rearrangements, and some taxa that retain IRs can also be extensively rearranged (e.g., Logacheva et al., 2014; Schelkunov et al., 2015).

The plastid rDNA gene *rrn*5, and the noncoding region between *rrn*23 and *rrn*4.5, have all been lost in *Pogoniopsis* (Table 1, Figure 1). The predicted loss of *rrn*5 has been reported in a few heterotrophic plants (Bellot and Renner, 2016; Arias-Agudelo et al., 2019; Su et al., 2019; Ceriotti et al., 2021; Yudina et al., 2021), but the functional significance of its absence has not been commented on. Continued function of the plastid ribosomal complex may require importation of an *rrn*5 homolog and possibly other ribosomal genes lost from the plastid genome (e.g., from the mitochondrion, or a nuclear transferred organellar gene), as suggested by Graham et al. (2017). The loss of the noncoding region between *rrn*23 and *rrn*4.5 resembles a return to the ancestral condition of the *rrn*23. In prokaryotes, sequence homologous to 4.5S starts the 23S gene (a ~100 bp gap was evidently introduced early in the evolution of land-plant plastids; MacKay, 1981).

Loss of introns

Retained plastid genes in *Pogoniopsis* have no *cis*-spliced introns (Table 1, Figure 1). Of the 17–20 introns normally present in the plastid genomes of land plants (Vogel et al., 1999; Bonen and Vogel, 2001), group IIA introns are typically found in eight plastid genes (one intron per gene in each of *atp*F, *clp*P, *trn*A-UGC, *trn*I-GAU, *trn*K-UUU, *trn*V-UAC, *rpl*2, and 3′-*rps*12; Zoschke et al., 2010; Wicke et al., 2011). The bulk of these introns are normally spliced by intron maturase K, coded for by the plastid *mat*K locus (e.g., Bonen and Vogel, 2001). In plants that retain introns in three of them—*clp*P, *rpl*2, and 3′-*rps*12—this maturase is not thought to be required for splicing of their group IIA introns (Zoschke et al., 2010; Graham et al., 2017; Barthet et al., 2020). Thus, although all three of these loci are retained in the *Pogoniopsis* plastome as intronless genes (Table 1, Figure 1), intron absence in them may be unrelated to retention vs. loss of *mat*K. However, because maturase K function is expected to be required if even one of the other five genes were retained, we predict that the *mat*K gene was lost in *Pogoniopsis* only after the loss of all five genes (i.e., *atp*F, *trn*A-UGC, *trn*I-GAU, *trn*K-UUU, *trn*V-UAC) and/or their introns (for these five genes, deletion of the genes would be expected following intron losses, to yield the observed pattern of gene retention in *Pogoniopsis*; Table 1).

The second intron typically present in *clp*P is a group IIB intron (it is the first of the two introns located in this gene) that relies on nuclear-encoded proteins for proper splicing (Asakura and Barkan, 2006); the *clp*P locus in *Pogoniopsis* has lost this intron too. The remaining genes containing *cis*-spliced introns in most flowering plants have all been lost in *Pogoniopsis*; these include another nine plastid genes with 10 additional group IIB introns, and a single plastid gene with a group I intron (see Table 1). However, while *P. schenckii* appears to represent an end stage of loss of *cis*-spliced introns in plastid genes, it may still retain *trans*-splicing of *rps*12, given that all three of its exons are present as open reading frames in *Pogoniopsis*. The *rps*12 exon 1 (i.e., 5′-*rps*12 in Figure 1) is normally *trans*-spliced to the distantly located 3′-*rps*12 transcript. In most plants, the latter transcript comprises exons 2 and 3 and a *cis*-spliced group IIA intron (also lost in *Pogoniopsis*; see above). *Rps*12 *trans*-splicing is not dependent on *mat*K, as the spliced region portions may be processed like an extended group IIB intron (e.g., Jenkins et al., 1997; Lee et al., 2019).

The primary mechanism for intron loss in plastid evolution is thought to be retroprocessing (i.e., with reverse transcription of a spliced mRNA to a cDNA, which then replaces the original genomic copy; Derr and Strathern, 1993; Odom and Herrin, 2013). Cuenca et al. (2016), investigated patterns of repeated retroprocessing in the mitochondrial genomes of Alismatales, a photosynthetic monocot order. However, this process has not been well explored in plastids, perhaps because intron loss is relatively rare in most angiosperm lineages and is typically limited to single genes (e.g., McPherson et al., 2004). It is not clear why four losses of *cis*-spliced introns have occurred in retained plastid genes in *Pogoniopsis* (i.e., *rpl*2, 3′-*rps*12, and both *clp*P introns). A general propensity for more elevated rates of evolution in heterotrophic lineages seems an inadequate explanation for this, given that there are no other major structural changes in the *Pogoniopsis* plastid genome, beyond gene/intron loss (Figure 3; Appendix S4), and that other heterotrophic lineages with substantial genomic rearrangements still retain plastid introns (e.g., Schelkunov et al., 2015; Su et al., 2019; Ceriotti et al., 2021; Yudina et al., 2021).

Loss of most tRNA genes and loss of function in bifunctional *trnE*

Most tRNA genes have been lost in *Pogoniopsis* (Table 1), consistent with some other fully mycoheterotrophic plants (e.g., Lam et al., 2015; Schelkunov et al., 2015; Lim et al., 2016). This may reflect a reliance on imported mitochondrial or nuclear encoded tRNAs to replace their function (e.g., Graham et al., 2017), although the mechanism for this still remains uncharacterized in plastids (Smith and Lee, 2014; Zoschke and Bock, 2018). The two retained plastid tRNA genes in *Pogoniopsis* (*trn*E-UUC and *trn*fM-CAU) are commonly observed in reduced plastid genomes of heterotrophic plants (e.g., Graham et al., 2017; Su et al., 2019; Ceriotti et al., 2021). The gene product of *trn*fM-CAU is the canonical initiator codon for translation in eubacteria and organelles and cannot normally be directly substituted by its cytosolic equivalent (Barbrook et al., 2006), although it has

been lost in other heterotrophic plants (e.g., Bellot and Renner, 2016; Arias-Agudelo et al., 2019; Su et al., 2019; Ceriotti et al., 2021; Yudina et al., 2021). Unusually, the *trn*E gene recovered from the *P. schenckii* plastome lacks the UUC-anticodon required to fulfill its normal function in translation (Figure 2), although it still retains a predicted cloverleaf structure. A similarly anticodon-less *trn*E has been reported in the plastid genomes of members of the endoparasitic family Balanophoraceae (Su et al., 2019; Ceriotti et al., 2021). The plastid *trn*E gene product is also known to play a secondary role in heme biosynthesis (Tanaka and Tanaka, 2007; Layer et al., 2010; see the pathway summarized in Appendix S13), and it appears that the canonical anticodon sequence is not required for the proper aminoacylation of *trn*E-Glu (Willows et al., 1995; Lüer et al., 2007). Thus, the apparent loss of translational function should not interfere with its role in the heme pathway, although this inference needs to be verified experimentally (e.g., Randau et al., 2004; Lüer et al., 2007).

CONCLUSIONS

After decades of debate regarding the systematic position of *Pogoniopsis* (reviewed by Cameron and van den Berg, 2017), the plastid and mitochondrial analyses here consistently place it within subfamily Epidendroideae. The use of mitochondrial genomic data sets to infer phylogenetic relationships in lineages that have very rapidly evolving plastid genomes was useful here, and should be useful in similar situations elsewhere, for example in other heterotrophic orchid lineages (Lam et al., 2018; Lin et al., 2022). The extreme plastid reduction found in *Pogoniopsis* due to gene loss mirrors its vegetative and reproductive structural changes (Alves et al., 2019, 2021), and is consistent with some other fully mycoheterotrophic lineages (e.g., Delannoy et al., 2011; Lam et al., 2015; Schelkunov et al., 2015; Petersen et al., 2018), although more gene loss was observed here than in most other mycoheterotrophs (see, e.g., Lam et al., 2018, app. S3). In the future, characterization of the nuclear genomes of *Pogoniopsis* and other heterotrophic lineages would be invaluable, to better understand the impact of loss of photosynthesis on other plastid functions, including translation and the myriad other biological processes that take place there (e.g., Yuan et al., 2018; Cai et al., 2021). It would be useful, for example, to look for possible functional transfer of translation apparatus genes to the nucleus. Regarding genes encoded in the plastome itself, we predict retention of only a few functions coded by the plastid genome beyond translation, such as the heme-biosynthesis functionality of plastid *trn*E. Retention of a handful of non-bioenergetic genes such as *acc*D and *trn*E has been hypothesized to explain plastid genome retention in other reduced heterotrophic lineages (e.g., Barbrook et al., 2006; Graham et al., 2017; Su et al., 2019). *Pogoniopsis* sets a current lower bound for the degree of plastid genomic reduction in orchids, consistent with the idea that plastid genome size is related to the degree of functional degradation (loss of function) following the loss of photosynthesis. The extreme reduction observed here points to *Pogoniopsis* being near the expected end point of genome reduction in heterotrophic plants (Barrett and Davis, 2012; Barrett et al., 2014; Wicke et al., 2016; Graham et al., 2017). However, despite extensive gene loss and loss of all *cis*-spliced introns in retained plastid genes, the plastid genome of *Pogoniopsis* is nearly colinear with autotrophic relatives, illustrating that different aspects of heterotrophic plastid genome degradation need not happen in lockstep. As an independently evolved fully mycoheterotrophic lineage, *Pogoniopsis* therefore adds significantly to our understanding of what happens when plants lose the capacity to photosynthesize.

AUTHOR CONTRIBUTIONS

Material collected and DNA extracted by J.L.S.M., D.S.S., F. Prosdocimi, and F. Pinheiro. N.J.K. performed contig assemblies, annotations/reannotations, and downstream analyses. N.J.K. and S.W.G. conceived the study and wrote the paper, with input on writing from all authors.

ACKNOWLEDGMENTS

The authors acknowledge that this work was partially completed on the unceded territory of the Coast Salish Peoples, including the territories of the xʷməθkʷəy̓əm (Musqueam), Sḵwx̱wú7mesh (Squamish), and səlilwətaɬ (Tsleil-Waututh) Nations. We thank two anonymous reviewers for their helpful comments; C. Furtado (Instituto Nacional de Cancer, INCA, Brazil) for genomic library preparation and sequencing on the Illumina HiSeq platform; and M. Soto Gomez (Royal Botanic Gardens, Kew, UK) for access to unpublished sequence information for six outgroup taxa in our phylogenetic analyses. Analyses were enabled in part by support provided by WestGrid (www.westgrid.ca) and the Digital Research Alliance of Canada (www.computecanada.ca). J.L.S.M. thanks the Conselho Nacional de Desenvolvimento Científico e Tecnológico (CNPq-303664/2020-7) and Fundação de Amparo à Pesquisa do Estado de São Paulo (FAPESP-2015/26479–6). This research was also supported by a FAPESP grant to F. Pinheiro (no. 16/22785-8; F. Pinheiro also acknowledges a productivity grant from CNPq, 302849/2021-1) and by a Natural Sciences and Engineering Research Council of Canada (NSERC) Discovery grant to S.W.G.

DATA AVAILABILITY STATEMENT

Sequence alignments are available on Figshare (https://figshare.com/s/4e693902cbf02ab33d3c for the plastid alignment; https://figshare.com/s/e58dd0a6666fbe4545d7 for the mitochondrial alignment). Newly generated sequences for *Pogoniopsis schenckii* are available on GenBank; plastid genome (OP425397), mitochondrial genes (OP434070–OP434076). Newly generated sequences for six outgroup taxa are also available on GenBank (OP434077–OP434315 and OP441128–OP441337).

ORCID

Nathaniel J. Klimpert http://orcid.org/0000-0003-0015-4045
Juliana Lischka Sampaio Mayer http://orcid.org/0000-0001-7439-5234
Deise Schroder Sarzi http://orcid.org/0000-0002-5658-7969
Francisco Prosdocimi http://orcid.org/0000-0002-6761-3069
Fábio Pinheiro http://orcid.org/0000-0003-3243-2652
Sean W. Graham http://orcid.org/0000-0001-8209-5231

REFERENCES

Alves, M. F., F. Pinheiro, M. P. Niedzwiedzki, and J. L. S. Mayer. 2019. First record of ategmic ovules in Orchidaceae offers new insights into mycoheterotrophic plants. *Frontiers in Plant Science* 10: 1447.

Alves, M. F., F. Pinheiro, C. E. P. Nunes, F. Prosdocimi, D. S. Sarzi, C. Furtado, and J. L. S. Mayer. 2021. Reproductive development and genetic structure of the mycoheterotrophic orchid *Pogoniopsis schenckii* Cogn. *BMC Plant Biology* 21: 1–14.

Angiosperm Phylogeny Group. 2003. An update of the Angiosperm Phylogeny Group classification for the orders and families of flowering plants: APG II. *Botanical Journal of the Linnean Society* 141: 399–436.

Angiosperm Phylogeny Group. 2009. An update of the Angiosperm Phylogeny Group classification for the orders and families of flowering plants: APG III. *Botanical Journal of the Linnean Society* 161: 105–121.

Angiosperm Phylogeny Group. 2016. An update of the Angiosperm Phylogeny Group classification for the orders and families of flowering plants: APG IV. *Botanical Journal of the Linnean Society* 181: 1–20.

Arias-Agudelo, L. M., F. González, J. P. Isaza, J. F. Alzate, and N. Pabón-Mora. 2019. Plastome reduction and gene content in New World *Pilostyles* (Apodanthaceae) unveils high similarities to African and Australian congeners. *Molecular Phylogenetics and Evolution* 135: 193–202.

Asakura, Y., and A. Barkan. 2006. *Arabidopsis* orthologs of maize chloroplast splicing factors promote splicing of orthologous and species-specific group II introns. *Plant Physiology* 142: 1656–1663.

Barbrook, A. C., C. J. Howe, and S. Purton. 2006. Why are plastid genomes retained in non-photosynthetic organisms? *Trends in Plant Science* 11: 101–108.

Barrett, C. F., and J. I. Davis. 2012. The plastid genome of the mycoheterotrophic *Corallorhiza striata* (Orchidaceae) is in the relatively early stages of degradation. *American Journal of Botany* 99: 1513–1523.

Barrett, C. F., J. Freudenstein, J. Li, D. R. Mayfield-Jones, L. Perez, J. C. Pires, and C. Santos. 2014. Investigating the path of plastid genome degradation in an early-transitional clade of heterotrophic orchids, and implications for heterotrophic angiosperms. *Molecular Biology and Evolution* 31: 3095–3112.

Barrett, C. F., and A. H. Kennedy. 2018. Plastid genome degradation in the endangered, mycoheterotrophic, North American orchid *Hexalectris warnockii*. *Genome Biology and Evolution* 10: 1657–1662.

Barrett, C. F., B. T. Sinn, A. H. Kennedy, and T. Pupko. 2019. Unprecedented parallel photosynthetic losses in a heterotrophic orchid genus. *Molecular Biology and Evolution* 36: 1884–1901.

Barthet, M. M., C. L. Pierpont, and E. K. Tavernier. 2020. Unraveling the role of the enigmatic MatK maturase in chloroplast group IIA intron excision. *Plant Direct* 4: e00208.

Bendich, A. J. 2004. Circular chloroplast chromosomes: the grand illusion. *The Plant Cell* 16: 1661–1666.

Bell, D., Q. Lin, W. K. Gerelle, S. Joya, Y. Chang, Z. N. Taylor, C. J. Rothfels, et al. 2020. Organellomic data sets confirm a cryptic consensus on (unrooted) land-plant relationships and provide new insights into bryophyte molecular evolution. *American Journal of Botany* 107: 91–115.

Bellot, S., and S. S. Renner. 2016. The plastomes of two species in the endoparasite genus *Pilostyles* (Apodanthaceae) each retain just five or six possibly functional genes. *Genome Biology and Evolution* 8: 189–201.

Bonen, L., and J. Vogel. 2001. The ins and outs of group II introns. *Trends in Genetics* 17: 322–331.

Bouman, F. 1984. The ovule. *In* B. M. Johri [ed.], *Embryology of Angiosperms*, 123–157. Springer, Berlin, Heidelberg.

Bromham, L., P. F. Cowman, and R. Lanfear. 2013. Parasitic plants have increased rates of molecular evolution across all three genomes. *BMC Evolutionary Biology* 13: 126.

Brown, R. H., D. L. Nickrent, and C. S. Gasser. 2010. Expression of ovule and integument-associated genes in reduced ovules of Santalales. *Evolution and Development* 12: 231–240.

Cai, L., B. J. Arnold, Z. Xi, D. E. Khost, N. Patel, C. B. Hartmann, S. Manickam, et al. 2021. Deeply altered genome architecture in the endoparasitic flowering plant *Sapria himalayana* Griff. (Rafflesiaceae). *Current Biology* 31: 1002–1011.e9.

Cameron, K. 2003. Vanilloideae. *In* A. M. Pridgeon, P. J. Cribb, M. W. Chase, and F. N. Rasmussen [eds.], *Genera Orchidacearum*, 281–334. Oxford University Press, Oxford.

Cameron, K. M., and C. van den Berg. 2017. *Pogoniopsis* is an epidendroid orchid that has been misclassified in subfamily Vanilloideae. *In* L. Campbell, J. I. Davis, A. W. Meerow, R. F. C. Naczi, D. W. Stevenson, and W. W. Thomas [eds.], *Diversity and Phylogeny of the Monocotyledons: Contributions from Monocots V (Memoirs of The New York Botanical Garden)*, 118.

Capella-Gutiérrez, S., J. M. Silla-Martínez, and T. Gabaldón. 2009. TrimAl: a tool for automated alignment trimming in large-scale phylogenetic analyses. *Bioinformatics* 25: 1972–1973.

Ceriotti, L. F., M. E. Roulet, and M. V. Sanchez-Puerta. 2021. Plastomes in the holoparasitic family Balanophoraceae: extremely high AT content, severe gene content reduction, and two independent genetic code changes. *Molecular Phylogenetics and Evolution* 162: 107208.

Chase, M. W., K. M. Cameron, J. Freudenstein, A. M. Pridgeon, G. Salazar, C. van den Berg, and A. Schuiteman. 2015. An updated classification of Orchidaceae. *Botanical Journal of the Linnean Society* 177: 151–174.

Cuenca, A., T. G. Ross, S. W. Graham, C. F. Barrett, J. I. Davis, O. Seberg, and G. Petersen. 2016. Localized retroprocessing as a model of intron loss in the plant mitochondrial genome. *Genome Biology and Evolution* 8: 2176–2189.

Darling, A. C. E., B. Mau, F. R. Blattner, and N. T. Perna. 2004. Mauve: multiple alignment of conserved genomic sequence with rearrangements. *Genome Research* 14: 1394–1403.

Darty, K., A. Denise, and Y. Ponty. 2009. VARNA: Interactive drawing and editing of the RNA secondary structure. *Bioinformatics* 25: 1974–1975.

Delannoy, E., S. Fujii, C. Colas des Francs-Small, M. Brundrett, and I. Small. 2011. Rampant gene loss in the underground orchid *Rhizanthella gardneri* highlights evolutionary constraints on plastid genomes. *Molecular Biology and Evolution* 28: 2077–2086.

Derr, L. K., and J. N. Strathern. 1993. A role for reverse transcripts in gene conversion. *Nature* 361: 170–173.

Dierckxsens, N., P. Mardulyn, and G. Smits. 2017. NOVOPlasty: de novo assembly of organelle genomes from whole genome data. *Nucleic Acids Research* 45: e18.

Doyle, J. J., and J. L. Doyle. 1990. Isolation of plant DNA from fresh tissue. *Focus* 12: 13–15.

Drouin, G., H. Daoud, and J. Xia. 2008. Relative rates of synonymous substitutions in the mitochondrial, chloroplast and nuclear genomes of seed plants. *Molecular Phylogenetics and Evolution* 49: 827–831.

Eddy, S. R. 1998. Profile hidden Markov models. *Bioinformatics* 14: 755–763.

Fejes, E., B. S. Masters, D. M. McCarty, and W. W. Hauswirth. 1988. Sequence and transcriptional analysis of a chloroplast insert in the mitochondrial genome of *Zea mays*. *Current Genetics* 13: 509–515.

Felsenstein, J. 1978. Cases in which parsimony or compatibility methods will be positively misleading. *Systematic Biology* 27: 401–410.

Felsenstein, J. 1985. Confidence limits on phylogenies: an approach using the bootstrap. *Evolution* 39: 783–791.

Feng, Y.-L., S. Wicke, J.-W. Li, Y. Han, C.-S. Lin, D.-Z. Li, T.-T. Zhou, et al. 2016. Lineage-specific reductions of plastid genomes in an orchid tribe with partially and fully mycoheterotrophic species. *Genome Biology and Evolution* 8: 2164–2175.

Freudenstein, J., and F. N. Rasmussen. 1999. What does morphology tell us about orchid relationships? A cladistic analysis. *American Journal of Botany* 86: 225–248.

Freudenstein, J. V., and M. W. Chase. 2015. Phylogenetic relationships in Epidendroideae (Orchidaceae), one of the great flowering plant radiations: progressive specialization and diversification. *Annals of Botany* 115: 665–681.

Gaut, B. S., and P. O. Lewis. 1995. Success of maximum likelihood phylogeny inference in the four-taxon case. *Molecular Biology and Evolution* 12: 152–162.

Givnish, T. J., D. Spalink, M. Ames, S. P. Lyon, S. J. Hunter, A. Zuluaga, W. J. D. Iles, et al. 2015. Orchid phylogenomics and multiple drivers of their extraordinary diversification. *Proceedings of the Royal Society B: Biological Sciences* 282: 20151553.

Givnish, T. J., A. Zuluaga, D. Spalink, M. S. Gomez, V. K. Y. Lam, J. M. Saarela, C. Sass, et al. 2018. Monocot plastid phylogenomics, timeline, net rates of species diversification, the power of multi-gene analyses, and a functional model for the origin of monocots. *American Journal of Botany* 105: 1888–1910.

Graham, S. W., V. K. Y. Lam, and V. S. F. T. Merckx. 2017. Plastomes on the edge: the evolutionary breakdown of mycoheterotroph plastid genomes. *New Phytologist* 214: 48–55.

Graham, S. W., P. A. Reeves, A. C. E. Burns, and R. G. Olmstead. 2000. Microstructural changes in noncoding chloroplast DNA: interpretation, evolution, and utility of indels and inversions in basal Angiosperm phylogenetic inference. *International Journal of Plant Sciences* 161: S83–S96.

Graham, S. W., J. M. Zgurski, M. A. Mcpherson, D. M. Cherniawsky, J. M. Saarela, et al. 2006. Robust inference of monocot deep phylogeny using an expanded multigene plastid data set. *Aliso* 22: 1–21.

Greiner, S., P. Lehwark, and R. Bock. 2019. OrganellarGenomeDRAW (OGDRAW) version 1.3.1: expanded toolkit for the graphical visualization of organellar genomes. *Nucleic Acids Research* 47: W59–W64.

Hendy, M. D., and D. Penny. 1989. A framework for the quantitative study of evolutionary trees. *Systematic Biology* 38: 297–309.

Ho, S. Y. W., and L. S. Jermiin. 2004. Tracing the decay of the historical signal in biological sequence data. *Systematic Biology* 53: 623–637.

Huo, X., Y. Zhao, Z. Qian, and M. Liu. 2018. Characterization of the complete chloroplast genome of *Eulophia zollingeri*, an endangered orchid in China. *Conservation Genetics Resources* 10: 817–819.

Jenkins, B. D., D. J. Kulhanek, and A. Barkan. 1997. Nuclear mutations that block group II RNA splicing in maize chloroplasts reveal several intron classes with distinct requirements for splicing factors. *Plant Cell* 9: 283–296.

Jiang, Y., X. Hu, Y. Yuan, X. Guo, M. W. Chase, S. Ge, J. Li, et al. 2022. The *Gastrodia menghaiensis* (Orchidaceae) genome provides new insights of orchid mycorrhizal interactions. *BMC Plant Biology* 22: 1–14.

Jost, M., J. Naumann, N. Rocamundi, A. A. Cocucci, S. Wanke, and A. A. C. Ar. 2020. The first plastid genome of the holoparasitic genus *Prosopanche* (Hydnoraceae). *Plants* 9: 306.

Joyce, E. M., D. M. Crayn, V. K. Y. Lam, W. K. Gerelle, S. W. Graham, and L. Nauheimer. 2018. Evolution of *Geosiris* (Iridaceae): Historical biogeography and plastid-genome evolution in a genus of non-photosynthetic tropical rainforest herbs disjunct across the Indian Ocean. *Australian Systematic Botany* 31: 504–522.

Kanehisa, M. 2019. Toward understanding the origin and evolution of cellular organisms. *Protein Science* 28: 1947–1951.

Kanehisa, M., M. Furumichi, Y. Sato, M. Ishiguro-Watanabe, and M. Tanabe, 2021. KEGG: integrating viruses and cellular organisms. *Nucleic Acids Research*. 49: D545–D551.

Kanehisa, M., and S. Goto. 2000. KEGG: Kyoto Encyclopedia of Genes and Genomes. *Nucleic Acids Research* 28: 27–30.

Katoh, K., and D. M. Standley. 2013. MAFFT multiple sequence alignment software version 7: improvements in performance and usability. *Molecular Biology and Evolution* 30: 772–780.

Kim, H. T., J. S. Kim, M. J. Moore, K. M. Neubig, N. H. Williams, W. M. Whitten, and J. H. Kim. 2015. Seven new complete plastome sequences reveal rampant independent loss of the *ndh* gene family across orchids and associated instability of the inverted repeat/small single-copy region boundaries. *PLoS One* 10: e0142215.

Kim, Y.-K., S. Jo, S.-H. Cheon, M.-J. Joo, J.-R. Hong, M. H. Kwak, and K.-J. Kim. 2019. Extensive losses of photosynthesis genes in the plastome of a mycoheterotrophic orchid, *Cyrtosia septentrionalis* (Vanilloideae: Orchidaceae). *Genome Biology and Evolution* 11: 565–571.

Kim, Y.-K., S. Jo, S.-H. Cheon, M.-J. Joo, J.-R. Hong, M. H. Kwak, and K.-J. Kim. 2020. Plastome evolution and phylogeny of Orchidaceae, with 24 new sequences. *Frontiers in Plant Science* 11: 22.

Knoop, V. 2004. The mitochondrial DNA of land plants: peculiarities in phylogenetic perspective. *Current Genetics* 46: 123–139.

Koressaar, T., and M. Remm. 2007. Enhancements and modifications of primer design program Primer3. *Bioinformatics* 23: 1289–1291.

Kosakovsky Pond, S. L., S. D. W. Frost, and S. V. Muse. 2005. HyPhy: Hypothesis testing using phylogenies. *Bioinformatics* 21: 676–679.

Kozik, A., B. A. Rowan, D. Lavelle, L. Berke, M. Eric Schranz, R. W. Michelmore, and A. C. Christensen. 2019. The alternative reality of plant mitochondrial DNA: one ring does not rule them all. *PLoS Genetics* 15: e1008373.

Kozlov, A. M., D. Darriba, T. Flouri, B. Morel, and A. Stamatakis. 2019. RAxML-NG: a fast, scalable and user-friendly tool for maximum likelihood phylogenetic inference. J. Wren [ed.]. *Bioinformatics* 35: 4453–4455.

Kuhner, M. K., and J. Felsenstein. 1994. A simulation comparison of phylogeny algorithms under equal and unequal evolutionary rates. *Molecular Biology and Evolution* 11: 459–468.

Lallemand, F., M. Logacheva, I. le Clainche, A. Bérard, E. Zheleznaia, M. May, M. Jakalski, et al. 2019. Thirteen new plastid genomes from mixotrophic and autotrophic species provide insights into heterotrophy evolution in Neottieae orchids. *Genome Biology and Evolution* 11: 2457–2467.

Lam, V. K. Y., H. Darby, V. S. F. T. Merckx, G. Lim, T. Yukawa, K. M. Neubig, J. R. Abbott, et al. 2018. Phylogenomic inference *in extremis*: a case study with mycoheterotroph plastomes. *American Journal of Botany* 105: 480–494.

Lam, V. K. Y., M. S. Gomez, and S. W. Graham. 2015. The highly reduced plastome of mycoheterotrophic *Sciaphila* (Triuridaceae) is colinear with its green relatives and is under strong purifying selection. *Genome Biology and Evolution* 7: 2220–2236.

Lam, V. K. Y., V. Merckx, and S. W. Graham. 2016. A few-gene plastid phylogenetic framework for mycoheterotrophic monocots. *American Journal of Botany* 103: 692–708.

Larsson, A. 2014. AliView: a fast and lightweight alignment viewer and editor for large datasets. *Bioinformatics* 30: 3276–3278.

Layer, G., J. Reichelt, D. Jahn, and D. W. Heinz. 2010. Structure and function of enzymes in heme biosynthesis. *Protein Science* 19: 1137–1161.

Lee, C., I. S. Choi, D. Cardoso, H. C. de Lima, L. P. de Queiroz, M. F. Wojciechowski, R. K. Jansen, and T. A. Ruhlman. 2021. The chicken or the egg? Plastome evolution and an independent loss of the inverted repeat in papilionoid legumes. *The Plant Journal* 107: 861–875.

Lee, K., S. J. Park, C. Colas des Francs-Small, M. Whitby, I. Small, and H. Kang. 2019. The coordinated action of PPR4 and EMB2654 on each intron half mediates *trans*-splicing of *rps*12 transcripts in plant chloroplasts. *The Plant Journal* 100: 1193–1207.

Lee, S. Y., K. Meng, H. Wang, R. Zhou, W. Liao, F. Chen, S. Zhang, and Q. Fan. 2020. Severe plastid genome size reduction in a mycoheterotrophic orchid, *Danxiaorchis singchiana*, reveals heavy gene loss and gene relocations. *Plants* 9: 521.

Lemaire, B., S. Huysmans, E. Smets, and V. Merckx. 2011. Rate accelerations in nuclear 18S rDNA of mycoheterotrophic and parasitic angiosperms. *Journal of Plant Research* 124: 561–576.

Li, L., B. Wang, Y. Liu, and Y.-L. Qiu. 2009. The complete mitochondrial genome sequence of the hornwort *Megaceros aenigmaticus* shows a mixed mode of conservative yet dynamic evolution in early land plant mitochondrial genomes. *Journal of Molecular Evolution* 68: 665–678.

Li, Y.-X., Z.-H. Li, A. Schuiteman, M. W. Chase, J.-W. Li, W.-C. Huang, A. Hidayat, S.-S. Wu, and X.-H. Jin. 2019. Phylogenomics of Orchidaceae based on plastid and mitochondrial genomes. *Molecular Phylogenetics and Evolution* 139: 106540.

Li, Z., Y. Jiang, X. Ma, J.-W. Li, J.-B. Yang, J.-Y. Wu, and X.-H. Jin. 2020. Plastid genome evolution in the subtribe Calypsoinae (Epidendroideae, Orchidaceae). *Genome Biology and Evolution* 12: 867–870.

Li, Z., X. Ma, Y. Wen, S. Chen, Y. Jiang, and X. Jin. 2020. Plastome of the mycoheterotrophic eudicot *Exacum paucisquama* (Gentianaceae) exhibits extensive gene loss and a highly expanded inverted repeat region. *PeerJ* 8: e9157.

Lim, G. S., C. F. Barrett, C. C. Pang, and J. I. Davis. 2016. Drastic reduction of plastome size in the mycoheterotrophic *Thismia tentaculata* relative to that of its autotrophic relative *Tacca chantrieri*. *American Journal of Botany* 103: 1129–1137.

Lin, Q., T. W. A. Braukmann, M. Soto Gomez, J. Lischka, S. Mayer, F. Pinheiro, V. S. F. T. Merckx, et al. 2022. Mitochondrial genomic data are effective at placing mycoheterotrophic lineages in plant phylogeny. *New Phytologist* 236: 1908–1921.

Liu, X., W. Fu, Y. Tang, W. Zhang, Z. Song, L. Li, J. Yang, et al. 2020. Diverse trajectories of plastome degradation in holoparasitic *Cistanche* and genomic location of the lost plastid genes. *Journal of Experimental Botany* 71: 877–892.

Logacheva, M. D., M. I. Schelkunov, M. S. Nuraliev, T. H. Samigullin, and A. A. Penin. 2014. The plastid genome of mycoheterotrophic monocot *Petrosavia stellaris* exhibits both gene losses and multiple rearrangements. *Genome Biology and Evolution* 6: 238–246.

Logacheva, M. D., M. I. Schelkunov, and A. A. Penin. 2011. Sequencing and analysis of plastid genome in mycoheterotrophic orchid *Neottia nidus-avis*. *Genome Biology and Evolution* 3: 1296–1303.

Lüer, C., S. Schauer, S. Virus, W. D. Schubert, D. W. Heinz, J. Moser, and D. Jahn. 2007. Glutamate recognition and hydride transfer by *Escherichia coli* glutamyl-tRNA reductase. *The FEBS Journal* 274: 4609–4614.

MacKay, R. M. 1981. The origin of plant chloroplast 4.5 S ribosomal RNA. *FEBS Letters* 123: 17–18.

von Martius, K. F. P., A. W. Eichler, I. Urban, S. Endlicher, E. Fenzl, B. Mary, and R. Oldenburg. 1893. Flora Brasiliensis, enumeratio plantarum in Brasilia hactenus detectarum:quas suis aliorumque botanicorum studiis descriptas et methodo naturali digestas partim icone illustratas. 4th ed. R. Oldenbourg, Munich & Leipzig.

McPherson, M. A., M. F. Fay, M. W. Chase, and S. W. Graham. 2004. Parallel loss of a slowly evolving intron from two closely related families in Asparagales. *Systematic Botany* 29: 296–307.

Merckx, V. S. F. T., F. T. Bakker, S. Huysmans, and E. Smets. 2009. Bias and conflict in phylogenetic inference of myco-heterotrophic plants: a case study in Thismiaceae. *Cladistics* 25: 64–77.

Merckx, V. S. F. T., and J. Freudenstein. 2010. Evolution of mycoheterotrophy in plants: a phylogenetic perspective. *New Phytologist* 185: 605–609.

Merckx, V. S. F. T., C. B. Mennes, K. G. Peay, and J. Geml. 2013. Evolution and diversification. *In* V. Merckx [ed.], *Mycoheterotrophy: The Biology of Plants Living on Fungi*, 215–244. Springer New York, New York, NY.

Miller, M. A., W. Pfeiffer, and T. Schwartz. 2010. Creating the CIPRES Science Gateway for inference of large phylogenetic trees. *In Proceedings of the Gateway Computing Environments Workshop (GCE)*, 14 Nov. 2010, New Orleans, LA, 1–8.

Mühlbauer, S. K., A. Lössl, L. Tzekova, Z. Zou, and H. U. Koop. 2002. Functional analysis of plastid DNA replication origins in tobacco by targeted inactivation. *The Plant Journal* 32: 175–184.

Naumann, J., J. P. Der, E. K. Wafula, S. S. Jones, S. T. Wagner, L. A. Honaas, P. E. Ralph, et al. 2016. Detecting and characterizing the highly divergent plastid genome of the nonphotosynthetic parasitic plant *Hydnora visseri* (Hydnoraceae). *Genome Biology and Evolution* 8: 345–363.

Nawrocki, E. P., and S. R. Eddy. 2013. Infernal 1.1: 100-fold faster RNA homology searches. *Bioinformatics* 29: 2933–2935.

Nguyen, L. T., H. A. Schmidt, A. von Haeseler, and B. Q. Minh. 2015. IQ-TREE: A fast and effective stochastic algorithm for estimating maximum-likelihood phylogenies. *Molecular Biology and Evolution* 32: 268–274.

Nickrent, D. L., A. Blarer, Y. L. Qiu, R. Vidal-Russell, and F. E. Anderson. 2004. Phylogenetic inference in Rafflesiales: the influence of rate heterogeneity and horizontal gene transfer. *BMC Evolutionary Biology* 4: 40.

Odom, O. W., and D. L. Herrin. 2013. Reverse transcription of spliced *psb*A mRNA in *Chlamydomonas* spp. and its possible role in evolutionary intron loss. *Molecular Biology and Evolution* 30: 2666–2675.

Oldenburg, D. J., and A. J. Bendich. 2004. Most chloroplast DNA of maize seedlings in linear molecules with defined ends and branched forms. *Journal of Molecular Biology* 335: 953–970.

Palmer, J. D. 1985. Comparative organization of chloroplast genomes. *Annual Review of Genetics* 19: 325–354.

Palmer, J. D. 1990. Contrasting modes and tempos of genome evolution in land plant organelles. *Trends in Genetics* 6: 115–120.

Palmer, J. D. 1991. Plastid chromosomes: structure and evolution. *In* L. Bogorad and I. K. Vasil [eds.], *The Molecular Biology of Plastids. Cell Culture and somatic Genetics of Plants* 7A: 5–53.

Palmer, J. D., and C. F. Delwiche. 1998. The origin and evolution of plastids and their genomes. *In Molecular Systematics of Plants II*: 375–409.

Palmer, J. D., and W. F. Thompson. 1982. Chloroplast DNA rearrangements are more frequent when a large inverted repeat sequence is lost. *Cell* 29: 537–550.

Pansarin, E. R. 2016. Recent advances on evolution of pollination systems and reproductive biology of Vanilloideae (Orchidaceae). *Lankesteriana* 16: 255–267.

Pansarin, E. R. 2021. Unravelling the enigma of seed dispersal in *Vanilla*. *Plant Biology* 23: 974–980.

Pansarin, E. R., A. Salatino, L. M. Pansarin, and M. Sazima. 2012. Pollination systems in Pogonieae (Orchidaceae: Vanilloideae): a hypothesis of evolution among reward and rewardless flowers. *Flora–Morphology, Distribution, Functional Ecology of Plants* 207: 849–861.

Pansarin, E. R., A. Salatino, and M. L. F. Salatino. 2008. Phylogeny of South American Pogonieae (Orchidaceae, Vanilloideae) based on sequences of nuclear ribosomal (ITS) and chloroplast (*psa*B, *rbc*L, *rps*16, and *trn*L-F) DNA, with emphasis on *Cleistes* and discussion of biogeographic implications. *Organisms Diversity & Evolution* 8: 171–181.

Pérez-Escobar, O. A., S. Dodsworth, D. Bogarín, S. Bellot, J. A. Balbuena, R. J. Schley, I. A. Kikuchi, et al. 2021. Hundreds of nuclear and plastid loci yield novel insights into orchid relationships. *American Journal of Botany* 108: 1166–1180.

Petersen, G., A. Cuenca, I. M. Møller, and O. Seberg. 2015. Massive gene loss in mistletoe (*Viscum*, Viscaceae) mitochondria. *Scientific Reports* 5: 1–7.

Petersen, G., H. Darby, V. K. Y. Lam, H. A. Pedersen, V. S. F. T. Merckx, A. Zervas, O. Seberg, and S. W. Graham. 2019. Mycoheterotrophic *Epirixanthes* (Polygalaceae) has a typical angiosperm mitogenome but unorthodox plastid genomes. *Annals of Botany* 124: 791–807.

Petersen, G., A. Zervas, H. Pedersen, and O. Seberg. 2018. Genome reports: contracted genes and dwarfed plastome in mycoheterotrophic *Sciaphila thaidanica* (Triuridaceae, Pandanales). *Genome Biology and Evolution* 10: 976–981.

Randau, L., S. Schauer, A. Ambrogelly, J. C. Salazar, J. Moser, S. I. Sekine, S. Yokoyama, et al. 2004. tRNA recognition by glutamyl-tRNA reductase. *Journal of Biological Chemistry* 279: 34931–34937.

Ranwez, V., E. J. P. Douzery, C. Cambon, N. Chantret, and F. Delsuc. 2018. MACSE v2: Toolkit for the alignment of coding sequences accounting for frameshifts and stop codons. *Molecular Biology and Evolution* 35: 2582–2584.

Raubeson, L. A., and R. K. Jansen. 2005. Chloroplast genomes of plants. *In* R. J. Henry [ed.], *Plant diversity and evolution: genotypic and phenotypic variation in higher plants*, 45–68. CABI, Wallingford UK.

Reichenbach, H. G. 1881. Otia botanica Hamburgensia. T.T. Meissneri, Hamburg.

Roquet, C., É. Coissac, C. Cruaud, M. Boleda, F. Boyer, A. Alberti, L. Gielly, et al. 2016. Understanding the evolution of holoparasitic plants: the complete plastid genome of the holoparasite *Cytinus hypocistis* (Cytinaceae). *Annals of Botany* 118: 885–896.

Sato, H. A., and A. M. Gonzalez. 2017. Embryogenesis, endospermogenesis and fruit development in *Lophophytum* (Balanophoraceae): focus on endosperm and embryo initiation. *Flora* 233: 79–89.

Scharff, L. B., and H. U. Koop. 2007. Targeted inactivation of the tobacco plastome origins of replication A and B. *The Plant Journal* 50: 782–794.

Schelkunov, M. I., V. Y. Shtratnikova, M. S. Nuraliev, M.-A. Selosse, A. A. Penin, and M. D. Logacheva. 2015. Exploring the limits for reduction of plastid genomes: a case study of the mycoheterotrophic orchids *Epipogium aphyllum* and *Epipogium roseum*. *Genome Biology and Evolution* 7: 1179–1191.

Serna-Sánchez, M. A., O. A. Pérez-Escobar, D., Bogarín, M. F. Torres-Jimenez, A. C. Alvarez-Yela, J. E., Arcila-Galvis, C. F. Hall, et al. 2021. Plastid phylogenomics resolves ambiguous relationships within the orchid family and provides a solid timeframe for biogeography and macroevolution. *Scientific Reports* 11: 6858.

Shen, X.-X., Y. Li, C. T. Hittinger, X. Chen, and A. Rokas. 2020. An investigation of irreproducibility in maximum likelihood phylogenetic inference. *Nature Communications* 11: 1–14.

Shtratnikova, V. Y., M. I. Schelkunov, A. A. Penin, and M. D. Logacheva. 2020. Mitochondrial genome of the nonphotosynthetic mycoheterotrophic plant *Hypopitys monotropa*, its structure, gene expression and RNA editing. *PeerJ* 2020: e9309.

Sisti, L. S., D. N. A. Flores-Borges, S. A. L. de Andrade, S. Koehler, M. L. Bonatelli, and J. L. S. Mayer. 2019. The role of non-mycorrhizal fungi in germination of the mycoheterotrophic orchid *Pogoniopsis schenckii* Cogn. *Frontiers in Plant Science* 10: 1589.

Smith, D. R., and R. W. Lee. 2014. A Plastid without a genome: evidence from the nonphotosynthetic green algal genus *Polytomella*. *Plant Physiology* 164: 1812–1819.

Soto Gomez, M., Q. Lin, E. da Silva Leal, T. J. Gallaher, D. Scherberich, C. B. Mennes, S. Y. Smith, and S. W. Graham. 2020. A bi-organellar phylogenomic study of Pandanales: inference of higher-order relationships and unusual rate-variation patterns. *Cladistics* 36: 481–504.

Steane, D. A., R. W. Scotland, D. J. Mabberley, and R. G. Olmstead. 1999. Molecular systematics of *Clerodendrum* (Lamiaceae): ITS sequences and total evidence. *American Journal of Botany* 86: 98–107.

Su, H. J., T. J. Barkman, W. Hao, S. S. Jones, J. Naumann, E. Skippington, E. K. Wafula, et al. 2019. Novel genetic code and record-setting AT-richness in the highly reduced plastid genome of the holoparasitic plant *Balanophora*. *Proceedings of the National Academy of Sciences of the United States of America* 116: 934–943.

Tanaka, R., and A. Tanaka. 2007. Tetrapyrrole biosynthesis in higher plants. *Annual Review of Plant Biology* 58: 321–346.

Tillich, M., P. Lehwark, T. Pellizzer, E. S. Ulbricht-Jones, A. Fischer, R. Bock, and S. Greiner. 2017. GeSeq–versatile and accurate annotation of organelle genomes. *Nucleic Acids Research* 45: W6–W11.

Tsukaya, H. 2018. How leaves of mycoheterotrophic plants evolved–from the view point of a developmental biologist. *New Phytologist* 217: 1401–1406.

Untergasser, A., H. Nijveen, X. Rao, T. Bisseling, R. Geurts, and J. A. M. Leunissen. 2007. Primer3Plus, an enhanced web interface to Primer3. *Nucleic Acids Research* 35: 71–74.

Vogel, J., T. Börner, and W. R. Hess. 1999. Comparative analysis of splicing of the complete set of chloroplast group II introns in three higher plant mutants. *Nucleic Acids Research* 27: 3866–3874.

Watanabe, S. 2013. A widely applicable bayesian information criterion. *Journal of Machine Learning Research* 14: 867–897.

Wertheim, J. O., B. Murrell, M. D. Smith, S. L. Kosakovsky Pond, and K. Scheffler. 2015. "RELAX: detecting relaxed selection in a phylogenetic framework." *Molecular Biology and Evolution* 32: 820–832.

Wheeler, D. L., D. M. Church, S. Federhen, A. E. Lash, T. L. Madden, J. U. Pontius, G. D. Schuler, et al. 2003. Database resources of the National Center for Biotechnology. *Nucleic Acids Research* 31: 28–33.

Wicke, S., K. F. Müller, C. W. DePamphilis, D. Quandt, S. Bellot, and G. M. Schneeweiss. 2016. Mechanistic model of evolutionary rate variation en route to a nonphotosynthetic lifestyle in plants. *Proceedings of the National Academy of Sciences* 113: 9045–9050.

Wicke, S., and J. Naumann. 2018. Molecular evolution of plastid genomes in parasitic flowering plants. *In* S.-M. Chaw and R. K. Jansen [eds.], *Advances in Botanical Research, Plastid Genome Evolution*, 315–347. Academic Press.

Wicke, S., G. M. Schneeweiss, C. W. dePamphilis, K. F. Müller, and D. Quandt. 2011. The evolution of the plastid chromosome in land plants: gene content, gene order, gene function. *Plant Molecular Biology* 76: 273–297.

Willows, R. D., C. Gamini Kannangara, and B. Pontoppidan. 1995. Nucleotides of tRNA (Glu) involved in recognition by barley chloroplast glutamyl-tRNA synthetase and glutamyl-tRNA reductase. *Biochimica et Biophysica Acta (BBA)–Gene Structure and Expression* 1263: 228–234.

Wolfe, K. H., W. H. Li, and P. M. Sharp. 1987. Rates of nucleotide substitution vary greatly among plant mitochondrial, chloroplast, and nuclear DNAs. *Proceedings of the National Academy of Sciences* 84: 9054–9058.

Yang, Z. 1998. Likelihood ratio tests for detecting positive selection and application to primate lysozyme evolution. *Molecular Biology and Evolution* 15: 568–573.

Yang, Z. 2007. PAML 4: phylogenetic analysis by maximum likelihood. *Molecular Biology and Evolution* 24: 1586–1591.

Yuan, Y., X. Jin, J. Liu, X. Zhao, J. Zhou, X. Wang, D. Wang, et al. 2018. The *Gastrodia elata* genome provides insights into plant adaptation to heterotrophy. *Nature Communications* 9: 1615.

Yudina, S. V., M. I. Schelkunov, L. Nauheimer, D. Crayn, S. Chantanaorrapint, M. Hroneš, M. Sochor, et al. 2021. Comparative analysis of plastid genomes in the non-photosynthetic genus *Thismia* reveals ongoing gene set reduction. *Frontiers in Plant Science* 12: 602598.

Zervas, A., G. Petersen, and O. Seberg. 2019. Mitochondrial genome evolution in parasitic plants. *BMC Evolutionary Biology* 19: 87.

Zhu, A., W. Guo, S. Gupta, W. Fan, and J. P. Mower. 2016. Evolutionary dynamics of the plastid inverted repeat: the effects of expansion, contraction, and loss on substitution rates. *New Phytologist* 209: 1747–1756.

Zoschke, R., and R. Bock. 2018. Chloroplast translation: structural and functional organization, operational control, and regulation. *The Plant Cell* 30: 745–770.

Zoschke, R., M. Nakamura, K. Liere, M. Sugiura, T. Börner, and C. Schmitz-Linneweber. 2010. An organellar maturase associates with multiple group II introns. *Proceedings of the National Academy of Sciences of the United States of America* 107: 3245–3250.

SUPPORTING INFORMATION

Additional supporting information can be found online in the Supporting Information section at the end of this article.

Appendix S1. List of primers used for confirming contig overlaps by Sanger sequencing.

Appendix S2. GenBank accession and publication source information for sequences used in phylogenetic inference.

Appendix S3. Optimal models and partitioning schemes for maximum likelihood phylogenetic analyses as inferred by IQ-TREE for DNA- and amino acid (AA)-based analyses.

Appendix S4. Mauve-based alignment of the plastome of *Pogoniopsis schenckii* with five autotrophic orchids.

Appendix S5. Phylogenetic relationship of *Pogoniopsis schenckii* with 274 other taxa inferred by an unpartitioned likelihood analysis of DNA sequences of 76 plastid genes.

Appendix S6. Phylogenetic relationship of *Pogoniopsis schenckii* with 274 other taxa inferred by a partitioned likelihood analysis of DNA sequences of 76 plastid genes.

Appendix S7. Phylogenetic relationship of *Pogoniopsis schenckii* with 274 other taxa inferred by an unpartitioned likelihood analysis of amino-acid sequences of 76 plastid genes.

Appendix S8. Phylogenetic relationship of *Pogoniopsis schenckii* with 274 other taxa inferred by a partitioned likelihood analysis of amino-acid sequences of 76 plastid genes.

Appendix S9. Phylogenetic relationship of *Pogoniopsis schenckii* with 68 other taxa inferred by an unpartitioned likelihood analysis of DNA sequences of 38 mitochondrial genes.

Appendix S10. Phylogenetic relationship of *Pogoniopsis schenckii* with 68 other taxa inferred by a partitioned likelihood analysis of DNA sequences of 38 mitochondrial genes.

Appendix S11. Phylogenetic relationship of *Pogoniopsis schenckii* with 68 other taxa inferred by an unpartitioned likelihood analysis of amino-acid sequences of 38 mitochondrial genes.

Appendix S12. Phylogenetic relationship of *Pogoniopsis schenckii* with 68 other taxa inferred by an partitioned likelihood analysis of amino-acid sequences of 38 mitochondrial genes.

Appendix S13. A simplified version of the heme biosynthesis pathway that begins with glutamate, showing the involvement of the plastid *trn*E-UUC gene product (i.e., L-Glutamyl-tRNA), based on entry ko01240 in the Kyoto Encyclopedia of Genes and Genomes (KEGG; Kanehisa and Goto, 2000; Kanehisa, 2019; Kanehisa et al., 2021).

How to cite this article: Klimpert, N. J., J. L. S. Mayer, D. S. Sarzi, F. Prosdocimi, F. Pinheiro, and S. W. Graham. 2022. Phylogenomics and plastome evolution of a Brazilian mycoheterotrophic orchid, *Pogoniopsis schenckii*. *American Journal of Botany* 109(12): 2030–2050.
https://doi.org/10.1002/ajb2.16084